12-2023

# Optimization of Hydraulic Cylinder Positioning for Wind Tower Hydraulic Erection System

Anbesh Rawal

THE UNIVERSITY OF NEWHAVEN

OPTIMIZATION OF HYDRAULIC CYLINDER POSITIONING FOR WIND TOWER
HYDRAULIC ERECTION SYSTEM

A THESIS

Submitted in partial fulfillment

of the requirements for the degree of

MASTER OF SCIENCE (Civil Engineering)

by

Anbesh Rawal

University of New Haven

West Haven, Connecticut

December 2023

OPTIMIZATION OF HYDRAULIC CYLINDER POSITIONING FOR WIND TOWER
HYDRAULIC ERECTION SYSTEM

APPROVED BY

Byungik Chang (Dec 12, 2023 09:29 EST)

_____

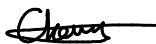Byungik Chang, Ph.D., P.E., M.B.A.
Thesis Adviser

Goli Nossoni (Dec 12, 2023 09:38 EST)

_____

Goli Nossoni, Ph.D.
Committee Member

_____

Nikodem Poplawski, Ph.D.
Committee Member

Byungik Chang (Dec 12, 2023 09:29 EST)

_____

Byungik Chang, Ph.D., P.E., M.B.A.
Program Coordinator

_____

Ronald Harichandran, Ph.D., P.E.
Dean of College of Engineering

_____

Nancy Savage, Ph.D.
Interim Provost

**ABSTRACT**

Wind produced electricity is a rapidly growing field with wind towers serving as critical components. Conventionally, special cranes are commonly used for wind tower erection. This study explores the use of hydraulic cylinders for small-scale wind tower erection. The thesis aims to find the optimal position of hydraulic cylinder connections in a hydraulic erection system for safe and energy-efficient tower erection and retraction and to enhance the performance and longevity of the system.

Structural analysis was conducted to investigate various hydraulic cylinder positioning configurations, ensuring minimal force exertion while maintaining structural integrity. The study included the selection of locally available hydraulic cylinders and the construction of a physical prototype of the hydraulic erection system to measure energy consumption.

This study sheds light on an alternative approach to small-scale wind tower erection, highlighting the significance of hydraulic cylinder positioning for safe and energy-efficient tower erection and retraction. The findings offer valuable insights for enhancing the wind energy sector's sustainability and performance.

The study identified the optimal connection point at 7.5 feet on the wind tower and 5 feet on the ground, away from the tower's base. Nevertheless, locally available hydraulic cylinders were found to be insufficient for the safe lowering of the tower, prompting the design of custom hydraulic cylinders to ensure both safety and economic feasibility.

# ACKNOWLEDGEMENT

I would like to express my heartfelt gratitude to the following individuals who have played a significant role in the completion of my thesis:

First and foremost, I want to thank my parents. Mom and Dad, your unwavering support, encouragement, and belief in me have been my pillars of strength throughout this journey. Your sacrifices and love have inspired me to reach for my goals, and I am forever grateful for everything you have done for me.

I extend my sincere appreciation to my thesis advisor, Professor Dr. Byungik Chang. Your guidance, expertise, and patience were instrumental in shaping my research and your mentorship has been invaluable, and I am fortunate to have had the opportunity to work under your supervision.

I want to acknowledge my roommates and friends, who have been my source of motivation and understanding during late nights and moments of frustration. Your support made this journey more enjoyable. Thank you for your encouragement, laughter, and occasional distractions that provided much-needed breaks from my work. Your friendship has been a source of inspiration and comfort.

This thesis would not have been possible without the support and encouragement of these wonderful individuals. I am deeply thankful for their contributions to my academic journey, and I look forward to the future with a heart full of gratitude.

**TABLE OF CONTENTS**

# LIST OF FIGURES

# LIST OF TABLES

CHAPTER 1: **INTRODUCTION**

1.1 BACKGROUND

Since the 1880s, coal and oil have been the primary sources of electricity, with coal alone

accounting for approximately 36% of global electricity generation. In the United States, coal

contributes to over 23.4% of the nation's electricity production. However, the use of coal is a

significant contributor to global temperature rise and poses environmental challenges. To address

these concerns, the United States has set ambitious developmental goals, aiming for renewable

energy sources to play a predominant role in the electricity sector by 2040 (Sørensen and

Sørensen, 2011).


Wind energy has emerged as a prominent renewable energy source, and its development has

gained significant momentum in the United States. The global wind energy statistics compiled by

the Global Wind Energy Council (GWEC) demonstrate a substantial increase in cumulative

installed wind capacity. In 1996, the capacity stood at 6.1 GW, and by 2015, it had reached 423.4

GW. This substantial growth reflects significant progress in wind energy system technology over

the past two decades. (Rashad et al., 2017)


Wind turbines towers are essential to wind energy productions. Since winds generally increase

with increasing altitude, larger blades and wind towers are preferred. As wind can flow more

freely at higher altitude, without much friction from trees and other obstructions, wind towers are

generally tall. The tower height is directly linked to the turbine rotor diameter, with the tower

height typically 1 to 1.5 times the rotor diameter. (Basu, 2010). Based on the height of the tower

and subsequently the rotor diameter, wind towers can be classified as Small (household),

Medium and Large. (Tummala et al., 2015). A classification of wind towers based on tower height is presented in Figure 1-1.
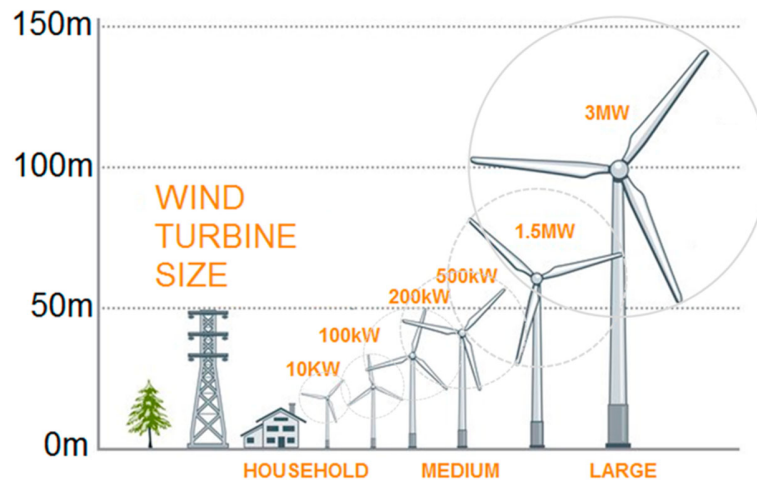


Figure 1-1 Size and capacity of different wind turbines (Calautit et al., 2018))

Several methods have been purposed for the erection of wind towers based on the type of tower. A lattice tower erection method has been proposed in which the tower is erected sectionally. A nacelle resting on a carrier is used to raise the second section with the first section already fixed to the foundation. (Von Ahn, 2012) Another method describes the wind tower to be erected by sections also with each section composed of a mantle plate which are sequentially arranged at the erection site. When the mantle plates are assembled, the section is attached to the lower end of the tower and another section is arranged likewise. (Trame and Müller, 2015)

A use of crane is the predominant method for wind tower erection. Cranes are not only necessary for erection but are also needed during the service stages for maintenance and replacing wind turbine equipment. Whether for tower erection or maintenance purposes, the high expenses

associated with crane operations pose a serious question to the economic viability of expanding wind energy projects. Figure 1-2 shows the Litronic tower crane erecting a wind turbine.



Figure 1-2 Litronic tower crane erects a wind turbine (Wind Power Engineering, 2016)

For small household wind turbine towers (10 – 98 ft) , the use of hydraulic cylinders dismisses the need for cranes and the cost associated with them offering as a promising alternative. By introducing a hinge joint slightly above the tower's base, wind turbines can be efficiently erected and lowered. An exact term for this method has not yet been proposed although this method has been seen used widely in the industry. This method will be referred to as hydraulic erection method in the study.

The position of the hydraulic cylinder in the hydraulic erection system has not yet been studied in detail. Optimal hydraulic cylinder positioning in the system can help ensure a safe and energy efficient erection process. The focus of this study is to investigate the structural integrity of a compact residential wind tower and its hydraulic cylinder, aiming to identify the most effective

positioning for enhancing safety and energy efficiency throughout the erection and lowering procedures.

The optimization of hydraulic cylinder positioning for wind tower erection holds significant promise for improving the efficiency, cost-effectiveness, and sustainability of wind energy projects. By addressing the challenges associated with crane-dependent construction methods, this research contributes to the continued growth and adoption of wind energy as a key component of the global renewable energy landscape.

## 1.2 RESEARCH SCOPE

In this thesis, the optimization of hydraulic cylinder positioning for wind tower erection is investigated. The research aims to enhance the performance, safety, and efficiency of wind tower construction by evaluating load distribution, determining optimal cylinder positions, and minimizing energy consumption. Through a combination of mathematical analysis and experimental testing, the study seeks to provide practical guidelines for selecting and positioning hydraulic cylinders in wind tower erection projects. The objectives of the research are :

- Calculate the required force exerted by hydraulic cylinders for safe and efficient wind tower erection.
- Assess the buckling strength of standard hydraulic cylinders and piston rods to determine their load-bearing capacities.
- Analyze the energy consumption of different hydraulic cylinder positions during the erection and lowering processes.

- Optimize hydraulic cylinder positioning to enhance load-bearing capacity, while minimizing energy consumption and operational costs.

- Provide design recommendations for custom hydraulic cylinders catering to the needs of this specific research.

## 1.3 THESIS OUTLINE

This thesis conducts an examination of optimizing hydraulic cylinder placement for wind tower erection. The research is organized into several chapters, each with specific objectives. The introductory chapter highlights the significance of the thesis and outlines research goals. The chapter also lays out research objectives, providing a clear roadmap for the study. Chapter 2 reviews pertinent literature, covering wind tower technologies, structural analysis, hydraulic systems, and energy consumption by hydraulic systems. The research methodology, including data collection, mathematical modeling, and prototype analysis are then discussed in Chapter 3. The chapter also navigates through the selection of hydraulic cylinders based on load-bearing capacity and structural requirements. Chapter 4 presents and discusses results, particularly focusing on energy efficiency, custom hydraulic cylinder design and optimal positioning. This chapter synthesizes the findings, drawing insightful conclusions about the optimal hydraulic cylinder positioning for wind tower erection. The last chapter concludes the study, summarizing key findings, discussing their implications for wind tower construction. This chapter offers recommendations for future work, highlighting potential areas for further research and improvement, ensuring the research's legacy continues to inform and guide advancements in wind tower erection practices.

CHAPTER 2: **LITERATURE REVIEW**

2.1 WIND TURBINE TECHNOLOGIES

Wind turbines play a pivotal role in harnessing the kinetic energy of wind and converting it into electrical power. This process is achieved through a straightforward mechanism: instead of using electricity to generate wind, as seen in conventional fans, wind turbines employ wind to generate electricity. Wind causes the blades of the turbine to rotate around a central rotor, which, in turn, powers a generator, producing electricity. (U.S. Department of Energy, 2014)

Wind turbines can be categorized based on the orientation of their axis installation. A horizontal axis wind turbine aligns its axis parallel to the ground, whereas a vertical axis wind turbine positions its axis perpendicular to the ground. Horizontal axis wind turbines offer several advantages, including enhanced efficiency, optimized wind speed utilization due to their height, and effective power regulation. However, horizontal axis wind turbines tend to be costlier compared to their vertical axis counterparts.

Selection of wind turbines depends upon the energy requirements. To meet the energy demands of an average home, which typically consumes about 10,649 kilowatt-hours (kWh) annually, a wind turbine rated in the range of 5 to 15 kW is necessary. For homes with a monthly consumption of 300 kWh in areas with an average wind speed of 14 mph (6.26 m/s), a 1.5-kW wind turbine is usually sufficient. (U.S. Energy Information Administration, 2023)

When considering small-scale household wind towers horizontal axis turbines are the most common. Also, since considering the household requirements a small-scale wind turbine is well

suited. A typical large-scale wind turbines has rotor diameters ranging from 50 m to 100 m and

power capacities ranging from 1 to 3 MW. In contrast, small-scale wind turbines feature rotor

diameters between 3 m and 10 m, offering power capacities of 1.4–20 kW which is more than

enough to meet home energy demands. (Tummala et al., 2015). Typically, small-scale wind

turbines feature a horizontal axis and consist of 2 to 3 fiberglass blades. While they may be

heavier, these turbines are engineered to deliver higher energy generation, making them the more

common choice for residential use. (Perch Energy, 2022)

Small-scale wind turbines and consequently household wind towers are selected for this thesis

because of the easy constructability, household use and accessibility, and economic viability.

The thesis centers on the utilization of hydraulic cylinders in the wind tower erection process,

aiming to enhance accessibility to wind energy for local communities. In this context, small-

scale household towers and turbines emerge as an ideal form factor for exploration. The focus is

on how hydraulic cylinders can play a pivotal role in the erection of these smaller structures,

contributing to the broader goal of making wind energy more attainable for local residents.

## 2.2 STRUCTURAL ANALYSIS OF A ROUND HOLLOW STEEL STRUCTURE

There are various forms of towers, lattice towers, concrete towers, tubular towers, and hybrid

towers that include a typical tower design. Although all forms of wind towers exist, the steel

tubular towers are the type most employed. Tubular towers are conical with their diameter

increasing toward the base. Taller towers required for larger diameters of their section to carry

their weight and in order to avoid structural failure. (Basu, 2010). Steel structures undergo failure

due to corrosion, reduction in strength when exposed fires, fatigue when loaded cyclically, and

buckling when under high compression and flexural stresses. Among these buckling is most common for all structures such as columns or towers.

Buckling is the sudden deformation or change in shape of a structural component. In the case of columns, tall columns may go through buckling if they do not possess sufficient sectional capacity to carry the weight. In case of a hydraulic system, the bending moment becomes the most significant since a large bending moment is generated at the point of connection with the hydraulic cylinder or at the tower base. It becomes important to check the tower against lateral torsional buckling. Lateral torsional buckling typically occurs in members with an asymmetric cross-section, such as I-beams or channels, where the combination of bending and twisting can lead to buckling. However, tubular wind towers are generally constructed with hollow steel members. In the case of hollow round steel sections, the absence of a distinct minor axis prevents the development of lateral torsional buckling. If a structural member lacks a distinct minor axis of bending, it suggests the cross-section of the member is symmetric or nearly symmetric about both axes. In such cases, the member primarily undergoes pure bending about its major axis. When a member experiences pure bending, the bending stresses are distributed uniformly across the cross-section, resulting in a simpler and more predictable behavior compared to members with asymmetric cross-sections. The absence of a minor axis of bending eliminates the possibility of lateral torsional buckling. This is the specific failure mode that occurs when both bending and twisting forces are present.

Without a minor axis of bending, the member's design and analysis become more straightforward. The structure either goes through yielding or local buckling. The buckling of hollow circular steel sections is discussed in Chapter F: Design of members for Flexure of the

AISC Steel Manual (American Institute of Steel Construction, 2017). Figure 2-1 shows the

failure of round tubes via local buckling as an example.



Figure 2-1 Failure of hollow tube due to Local buckling (Adbulla, 2021).

Based on the AISC Specification for Structural Steel Buildings, the classification and design of

round hollow steel structures follow specific guidelines. To qualify as a round hollow steel

structure, the ratio of the outer diameter (D) to the thickness (t) must satisfy Equation

2.1. (American Institute of Steel Construction, 2017)

$$\frac{D}{t} = \frac{0.45E}{F_y} \qquad (2.1)$$

where E is the modulus of elasticity, D is the outer diameter at the section, t is the thickness of

the section walls and $F_y$ is the material yield strength.

Once classified, the nominal flexural strength ($M_n$) is determined as the lesser of the yielding

limit state (plastic moment) and the local buckling strength. The yielding limit state is calculated

using Equation 2.2.

$$M_n = M_p = F_y Z \tag{2.2}$$

where Z is the plastic modulus of the member's cross section.

For local buckling, the section must be confirmed as either compact, non-compact or slender based on Table B4.1b of the AISC Specification. Compact sections' limit state of flange buckling is non-existent. For non-compact sections however, Equation 2.3 is utilized.

$$M_n = \left[ \frac{0.021E}{\frac{D}{t}} + F_y \right] \times S \tag{2.3}$$

Where S is the elastic modulus of member cross section

Similarly, Equation 2.4 gives the nominal moment capacity for sections judged to have slender walls.

$$M_n = F_{cr} S \tag{2.4}$$

where,

$$F_{cr} = \frac{0.33E}{\frac{D}{t}} \tag{2.5}$$

$F_{cr}$ is the critical stress and $M_n$ is the nominal moment capacity.

## 2.3 HYDRAULIC LIFTING SYSTEMS

Hydraulics play an important role in various lifting systems, providing efficient and reliable means of raising heavy loads. Whether in construction equipment, industrial machinery, or automotive applications, hydraulic lifting systems offer several advantages.

Hydraulic lifting systems commonly employ hydraulic cylinders or rams to generate the necessary force for lifting heavy objects. These systems operate based on Pascal's principle, where pressure applied to a confined fluid is evenly transmitted in all directions.

### 2.3.1 VEHICLE MOUNTED MISSILE SYSTEMS

Hydraulic cylinders are essential components in vehicle-mounted missile launchers, serving multiple essential functions. They are essential in erecting the missile, adjusting the launch angle, stabilizing the launcher platform, absorbing recoil forces, and controlling the missile release. These cylinders provide the necessary force, control, and stability for successful missile deployment. They enable the smooth and precise movement of the missile, ensuring accurate targeting and trajectory control. Additionally, hydraulic cylinders absorb the significant recoil forces generated during launch, protecting the launcher structure. A vehicle-mounted missile system is depicted in a simplified diagram in Figure 2-2.
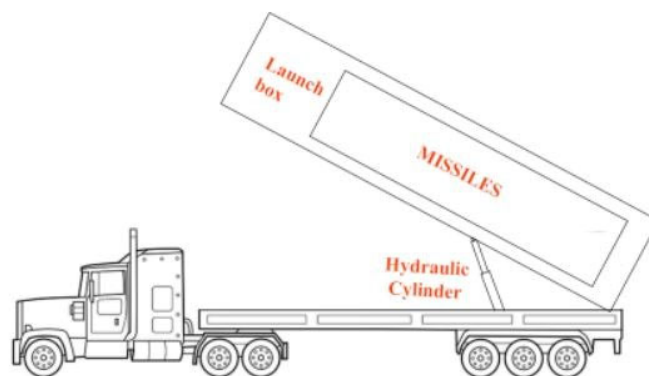


Figure 2-2 Vehicle mounted missile system.

Numerous research efforts have been conducted to determine the stability of this hydraulic system. Research on the coupling effect of the erecting process (Wei et al., 2016) acknowledges the importance of the erecting process in missile launch systems and the need for improvements in speed and smoothness. The study outlines the components of vehicle-mounted missile systems, including mechanical, hydraulic, and electrical systems. It emphasizes the role of hydraulic cylinders in the erecting process, stating that these cylinders are important for lifting and positioning the missile. The friction and collision forces experienced by the cylinders are also discussed, highlighting the significance of accurate dynamic modelling to ensure smooth and stable movement.

Hydraulic missile erecting systems serve as a relevant and illustrative example for the hydraulic erection system to be discussed in this thesis. These systems offer valuable insights into various aspects, including stability analysis and other relevant factors specific to hydraulic systems. By examining the dynamics and performance of hydraulic systems in missile erecting processes a deeper understanding of their stability characteristics and other associated phenomena can be gained.

2.3.2 TELESCOPIC WIND STEEL POLES

Wind farms have gained considerable attention in the renewable energy sector, but their conventional design poses environmental challenges such as landscape alteration, risks to wildlife, noise pollution, and the disposal of mechanical components. The PERIMA project proposed the design and construction of a prototype for an extendable and self-erecting wind pole, specifically targeting the commercial sector of mini-wind farms. The prototype presented in

Figure 2-3 features a 60-kilowatt wind turbine mounted atop a 30-meter-high pole, incorporating a unique hydraulic lifting system (Campione et al., 2021).
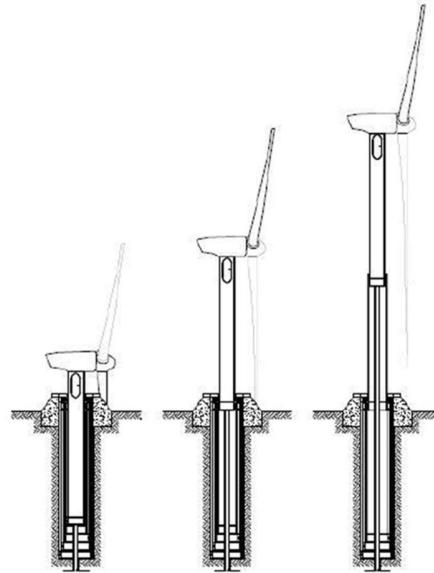


Figure 2-3 Hydraulic cylinders used to lift telescopic towers (Campione et al., 2021)

The telescopic wind pole shown above in figure 2-3 incorporates a hydraulic mechanism allowing the pole to be lowered and raised. When in the rest position, the telescopic structure is housed inside a foundation pit, and the wind turbine's propeller remains horizontally positioned close to the ground. Inspired by the lifting system of jack-up rigs, which are mobile platforms capable of elevating their hulls above the surface of the sea, the lifting system of the prototype wind pole employs a similar principle. Specifically, it utilizes hydraulic pistons to raise a steel piston located internally and coaxially within the wind pole, thus enabling the extension of the telescopic tower to its maximum erection position (Campione et al., 2021)

The lifting system in the suggested prototype consists of a steel piston connected to hydraulic cylinders, which drag the three segments of the wind pole to the desired height of 30 m.

Buckling strength of the hydraulic lifting steel tube was studied and useful conclusions were made with regards to its applicability.

The hydraulic lifting system employed in the PERIMA project's wind pole provides a practical case study for studying hydraulic erection systems. The system's performance, structural integrity, and efficiency can be examined under varying loads and environmental conditions. Findings from this study can contribute to the development of more efficient and reliable hydraulic lifting systems in various applications.

### 2.3.3 TRUCK CRANES/ DUMP TRUCKS

Truck cranes are widely utilized in industries such as construction, logistics, and transportation for lifting and moving heavy loads. These cranes rely on hydraulic systems to provide the necessary power and control for their lifting operations. Figure 2-4 depicts a straightforward representation of a working dump truck featuring a telescopic cylinder.
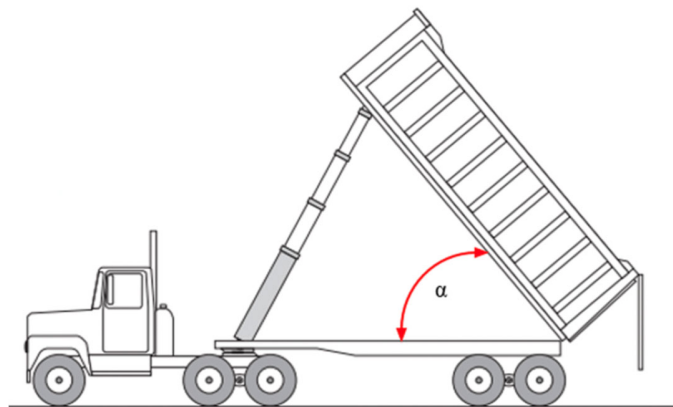


Figure 2-4 A Dump-truck with telescopic cylinder (Solazzi and Buffoli, 2019)

Hydraulic systems in truck cranes consist of hydraulic cylinders, pumps, valves, and fluid reservoirs. The hydraulic cylinders are responsible for generating the lifting force, while the

pumps supply pressurized hydraulic fluid to the cylinders. Valves regulate the flow of hydraulic fluid, enabling precise control of the crane's movements.

The hydraulic system allows for the smooth and controlled operation of the crane's boom, allowing it to extend, retract, and rotate. It also enables precise positioning of the load, ensuring stability and safety during lifting operations. The hydraulic system's ability to transmit high forces and operate efficiently makes it an ideal choice for truck cranes.

Sochacki (2007) uses a physical model for testing the dynamics of the truck crane in this study, which is a laboratory-scale representation of a real truck crane. The model incorporates hydraulic systems to control all operational motions. Various factors (i.e., the reacting force of the load, the system's geometry defined by angles, and the equivalent masses and rigidity of the boom) are considered in the physical model.

A similar approach has been utilized in this thesis for the lifting mechanism of a hydraulic erection system. Although Sochacki's study focuses on the stability analysis of a truck crane, it provides valuable insights into the importance of stability considerations in mechanical systems. Wind towers, especially self-erecting ones, need to be structurally stable during the erection process and in operational conditions.

## 2.4 BUCKLING AND BUCKLING BEHAVIOR OF HYDRAULIC CYLINDER

Buckling is the sudden change in shape of a structural component under load. The typical forms of steel member buckling commonly considered in structural design encompass lateral-torsional

buckling and local buckling modes. Lateral-torsional buckling entails the translation and twisting of the member's cross-sections as rigid entities. Conversely, local buckling is distinguished by localized distortions in the cross-section occurring over a short span without lateral translation.

These two modes represent the primary forms of buckling. Local buckling predominating in the case of shorter members and lateral-torsional buckling is more prevalent in longer members. For members of intermediate length, a combined effect emerges, resulting in lateral-distortional buckling. This type of buckling is characterized by concurrent distortion and lateral deflection of the cross-section. (Bradford, 1992)

Buckling strength is an important requirement for hydraulic cylinders, and engineers have been using Euler's equation, which describes buckling as an elastic instability, since 1744. However, for smaller slenderness structures with non-linear behavior of material and or imperfections of geometry and load, Euler's method has demonstrated incapability to predict critical loads for structures to overcome the deficiencies of Euler's method, various theoretical and empirical approaches have been developed. Recent research has focused on estimating the buckling load capacity of hydraulic cylinders, considering factors often neglected by industry designers, such as friction at supports, misalignments at junctions, wear of materials, and internal pressure. (Narvydas, 2017). Figure 2-5 visually demonstrates the occurrence of buckling in a typical hydraulic cylinder.
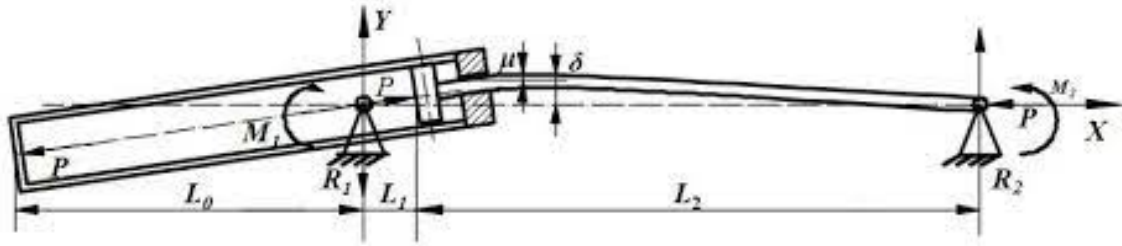
Figure 2-5 Buckling failure of a regular hydraulic cylinder (Xiong-Hao et al.,2017).

## 2.4.1 INDUSTRIAL SPECIFICATIONS

Industries present various methods for calculating the buckling strength of a hydraulic cylinder, often supplying customers with charts or tables to help them identify the hydraulic cylinder suitable for their requirements.

These calculations are based on Euler's equation presented in Equation 2.6.

$$P_{cr} = \frac{\pi^2 \times E \times I}{nL_e} \qquad (2.6)$$

when $\lambda > \lambda_{cr}$

In the above equations, E represents the modulus of elasticity of the rod material, I denotes the geometric moment of inertia for a solid circular cross-section ($\frac{\pi d^4}{64}$, where d is the diameter of the piston rod), $L_e$ is the effective length depending on the type of mounting, n is the safety factor, $\lambda$ is the slenderness ratio ($\lambda = \frac{4L_k}{d}$), and $\lambda_{cr}$ is the critical slenderness ratio ($\lambda_{cr} = \pi \sqrt{\frac{E}{0.8R_e}}$)

It should be noted that the above method only takes into account the diameter of the piston rod, making it a simple and convenient approach for engineering applications. Models representing the hydraulic cylinder solely based on the cross-section of the piston rod are referred to as RD (rod diameter) models in this context.

In the DNV-GL class guideline for hydraulic cylinders and the DNV standard for certification of hydraulic cylinders, a different buckling calculation method is provided. The buckling load is calculated using Equation 2.7. (Narvydas, 2017)

$$P_e = \frac{\pi^2 E}{LZ} \tag{2.7}$$

where L is the total length of the hydraulic cylinder between mountings in the fully extracted position. Z is a parameter calculated in equation 2.8 dependent on the moments of inertia of the cylinder tube ($I_1$) and piston rod ($I_2$), as well as the length of the cylinder tube part ($L_1$) and the length of the piston rod ($L_2$) in the fully extracted position.

$$Z = \frac{L_1}{I_1} + \frac{L_2}{I_2} + \left(\frac{1}{I_2} - \frac{1}{I_1}\right) \times \frac{L}{2\pi} \times sin\left(2\pi \times \frac{L_1}{L}\right) \tag{2.8}$$

This approach considers not only the diameter and stroke length of the piston rod but also the cross-section and length of the cylinder tube. (Narvydas, 2017)

### 2.4.2 LONG CYLINDERS

The analysis of stress, deflection, and buckling tendency in hydraulic cylinder piston rods is a complex task, and various methods and formulas have been developed for this purpose. However, many of these methods provide results differing significantly from observed field and laboratory data. The need for a reliable structural analysis technique in hydraulic cylinder design is widely recognized, particularly in applications where cylinders are pushed to their limits to reduce cost, optimize material usage, and save weight.

Parrett and Iyengar (1976) studied a method developed for the structural study of long hydraulic cylinders called "SACREG" (structural analysis of regular hydraulic cylinders). It was developed as part of the cylinder integrity assessment project conducted at the Fluid Power Research Center of Oklahoma State University, sponsored by the U.S. Army MERDC and several industrial firms. Traditionally, cylinder rod sizing against buckling failure has relied on the Euler formula and its variations. However, this approach often overlooks important factors and treats the hydraulic cylinder as a self-contained pressure vessel, neglecting the actual behavior of the cylinder and rod interface. The hydrostatic forces in the longitudinal direction of the cylinder are transmitted to the pins through the piston and end cap, eliminating the need for axial stresses.

With the demand for long stroke cylinders, telescopic cylinders, and non-conventional designs requiring high strength-to-weight and stiffness-to-weight ratios, a more precise analysis is necessary. The refined analysis takes into account factors such as clearances at the piston head and gland, compressibility of seals and bearings, eccentricity of axial load, self-weight of the cylinder and rod, friction at supporting pins, and support locations and end conditions. The SACREG analysis is based on the fundamental equation relating the bending moment of a straight elastic beam to its curvature. By integrating this equation and considering appropriate end conditions, the deflection curve and maximum deflections can be determined, along with the location and magnitude of maximum stresses. The objective is to determine the maximum safe load that satisfies design requirements, such as not exceeding the yield strength of materials or prescribed deflection limits.

Due to the complexity of the calculations, computer algorithms are used to perform the calculations which takes into account factors such as crookedness angle, deflections, and stresses caused by clearances, compressibility, eccentricity, self-weight, friction, and support conditions.

In summary, analyzing long hydraulic cylinders requires a comprehensive approach considering multiple failure modes, the flexibility of the cylinder rod interface, and various external factors. The SACREG method provides a refined structural analysis technique, enabling engineers to optimize designs by considering the effects of stroke length, mounting position, and other design parameters on stresses, deflections, internal bearing loads, and the critical axial load.

### 2.4.3 TELESCOPIC HYDRAULIC CYLINDERS

The design of multistage hydraulic cylinders, also known as telescopic cylinders, requires an understanding of the buckling load, which is a necessary parameter. However, there are limited methods available for analyzing the buckling load of hydraulic cylinders.

Telescopic hydraulic cylinders are widely utilized as linear actuators, especially in applications like cargo trucks requiring a substantial moving span exceeding the length of the closed device. However, during the active phase of actuation, these cylinders face external compressive loadings in increasingly slender configurations, which can lead to buckling failures. (Aggressive Hydraulic, 2023) Understanding the buckling behavior of telescopic hydraulic cylinders is major to ensure their safe and efficient operation. A conventional telescopic hydraulic cylinder is illustrated in Figure 2-6.

Figure 2-6 Telescopic hydraulic cylinder (Apex Hydraulics, 2016)

To investigate the buckling phenomenon, experimental measurements have been conducted on telescopic cylinders in both laboratory settings and real operational conditions. The focus of the study was on limiting axial loadings of fully extended cylinders. During the experiments, strains of the material in critical sections and the lateral deflections of the tested structures were recorded, taking into account the applied loads. By analyzing the obtained data, Wangikar et al., (2015) aimed to identify the signs of incipient buckling and assess the ultimate load carrying capabilities of these components. Buckling failures in telescopic cylinders, especially when extended, were found to be responsible for critical accidents in various applications. The primary causes of such failures are often attributed to axial overloading or excessive lateral inclination of the lifting devices. Figure 2-7 show the buckling analysis of a long telescopic hydraulic cylinder carried out in ANSYS for research.
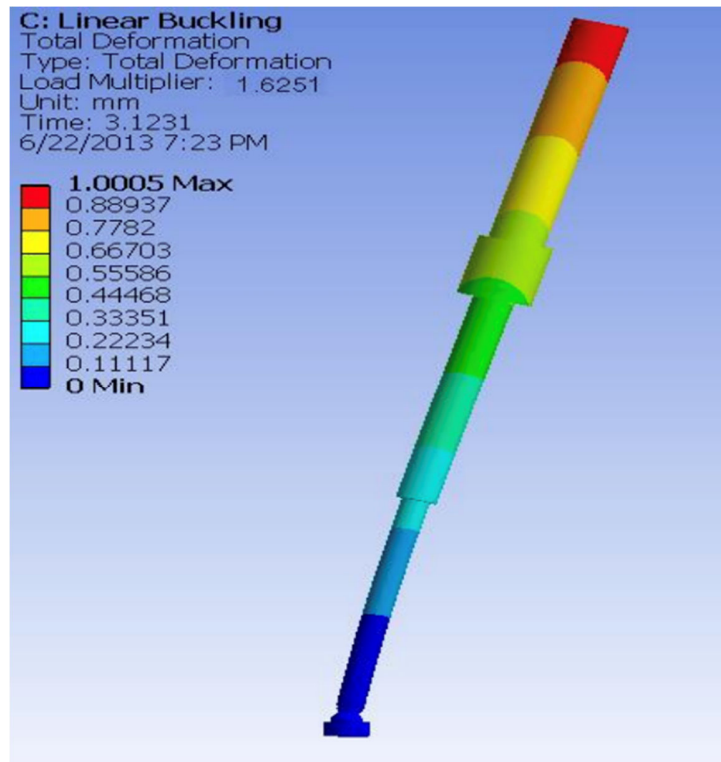
Figure 2-7 Linear buckling analysis of telescopic hydraulic cylinder (Wangikar et al., 2015)

Many numerical methods have been proposed to estimate the ultimate buckling loads, relying solely on calculations may introduce errors due to shape and geometric tolerances, as well as uncertainties in evaluating junction stiffness. Therefore, conducting experimental investigations is pivotal for accurately assessing the performance and safety of telescopic cylinders. (Wangikar et al., 2015)

One example of experimental measurements involved a workshop scenario where the buckling load of a 6-element telescopic cylinder was evaluated by Morelli (2009). The cylinder was extended to a length of 11.2 meters and secured to a rigid test bench using hinges at both ends. Load was applied using a manual hydraulic pump, and the resulting axial load was transduced through a digital pressure gauge. Morelli also carried out field experimentation using a 5-element

22

telescopic cylinder installed in a heavy-duty transport truck. Strain gauges were applied to the cylinder, enabling the measurement of transverse and longitudinal bending moments during operation. The cylinder was subjected to various operating conditions, simulating critical scenarios where the truck's rear frame was laterally inclined, and the cargo was lifted without being discharged.

The experiment revealed significant buckling deflections, which induced progressive elongations of the cylinder. Observations revealed an increase in the internal volume of the cylinder, resulting in a reduction in oil pressure and axial load. Although this effect improved the safety of the experimental procedures, practical applications of lifting devices driven by external loads would likely result in abrupt collapses of the structure when buckling occurs. (Morelli, 2009)

The strain energy method and weighted moment of inertia method are compared using ANSYS finite element analysis to determine the critical buckling load of a typical multistage hydraulic cylinder. This comparison provides insights into the accuracy and applicability of these methods.

The research by Valliappan and Basha (2017) focused on the strain energy method and weighted moment of inertia method for calculating the critical buckling load of multistage hydraulic cylinders. The strain energy method, based on Timoshenko's work (Timoshenko,1963), equates the potential energy (DT) to the strain energy (DU) for the same force and displacement. By considering the strain energy, the critical buckling load (P) can be obtained using the equations provided. It assumes certain Euler-Bernoulli's assumptions, such as homogeneous and isotropic material, plane sections remaining plane after loading, and negligible transverse shear.

The weighted moment of inertia method, on the other hand, provides an approximate solution for long slender non-prismatic columns. It is used to calculate the critical load based on the weighted moment of inertia, which considers the moment of inertia of each section and its length. The buckling load in each condition is calculated using the following equations.

For hinged Multistage Cylinder

$$P = \frac{\pi^2 E}{2L_n\left\{\sum_{i=1}^{n}\frac{Z_i}{I_i}\right\}}$$  (2.9)

For Fixed Free Mounting Multistage Cylinder

$$P = \frac{\pi^2 E}{8L_n\left\{\sum_{i=1}^{n}\frac{Z_i}{I_i}\right\}}$$  (2.10)

For Multistage Cylinder Using Weighted Moment of Inertia

$$P = \frac{\pi^2 E I_o}{4L_n^2}$$  (2.11)

Here $L_n$ is the total length, Z is a parameter that depends on length and moment of inertia, I is the moment of inertia and P is the buckling force.

To validate the strain energy method and weighted moment of inertia method, finite element analysis using ANSYS software was performed. The critical buckling load obtained from these methods was compared to the results obtained from the finite element analysis. The accuracy and reliability of the strain energy and weighted moment of inertia methods can be checked using this approach and a comparison can be made.

## 2.5 ENERGY EFFICIENCY AND CALCULATIONS IN HYDRAULIC SYSTEMS

Calculating the energy on a curved path requires considering both the potential energy and the kinetic energy of the object moving along the curve. The potential energy is associated with the object's position relative to a reference point, while the kinetic energy is associated with its motion.

The potential energy is determined by the object's height above a chosen reference point. If the curved path is in a gravitational field, the potential energy (PE) can be calculated using Equation 2.12.

$$PE = m \times g \times h \qquad (2.12)$$

where m is the mass of the object, g is the acceleration due to gravity, and h is the vertical distance above the reference point.

Next, the kinetic energy of the object along the curved path is calculated. Kinetic energy is related to the object's mass and its velocity.

To account for the changes in potential and kinetic energy along the curved path, one must analyze the variations in height and velocity at different points. At each point on the curve, the potential and kinetic energy values are calculated, and the sum of these energies represents the total energy at that point. By repeating this process for various points along the curve, an understanding of the energy distribution and changes throughout the path can be obtained.

## 2.6 BASIC HYDRAULIC FORMULA FROM MANUFACTURERS

Manufacturers and designers have provided a list of general formulas for calculating various hydraulic parameters. These parameters are useful to calculate the energy consumed by hydraulic cylinder. Common hydraulic formulas used in the industry are tabulated in Table 2-1.

Table 2-1 Industrial hydraulic formulas (Aggressive Hydraulics, 2019 and Flodraulic, 2019)

| | | |
|---|---|---|
| Extend Area (in²) | = | $\frac{\pi}{4} \times Bore\ Diameter^{\,2}$ |
| Extend Volume (in³) | = | $\frac{\pi}{4} \times Bore\ Diameter\ (in)^2 \times Stroke\ (in)$ |
| Extend Time (sec) | = | $\frac{(Extend\ Volume\ (in^3) \times 60)}{(Flow\ (gpm) \times 231)}$ |
| Extend Rate (in/sec) | = | $\frac{Flow\ (gpm) \times 231}{Extend\ Area\ (in^2) \times 60}$ |
| Extend Force (lbs) | = | $Extend\ Area\ (in^2) \times Pressure\ (psi)$ |
| Retract Area (in²) | = | $\frac{\pi}{4} \times (Bore\ Diameter\ (in)^2 - Rod\ Diameter\ (in)^2)$ |
| Retract Volume (in³) | = | $\frac{\pi}{4} \times (Bore\ Diameter\ (in)^2 - Rod\ Diameter\ (in)^2) \times Stroke$ |
| Retract Time (sec) | = | $\frac{Retract\ Volume\ (in^3) \times 60}{Flow\ (gpm) \times 231}$ |
| Retract Rate (in/sec) | = | $\frac{Flow\ (gpm) \times 231}{Retract\ Area \times 60}$ |
| Retract Force (lbs) | = | $Retract\ Area\ (in^2) \times Pressure\ (psi)$ |

| | | |
|---|---|---|
| Cylinder Ratio | = | $\dfrac{Extend\ Area\ in^2}{Retract\ Area\ (in^2)}$ |
| Flow out rod (gpm) | = | $\dfrac{Flow\ in\ base\ (gpm)}{Cylinder\ Ratio}$ |
| Flow out base (gpm) | = | $Flow\ in\ rod\ (gpm)\ \times\ Cylinder\ Ratio$ |

CHAPTER 3: **METHODOLOGY**

This chapter describes the methods employed to achieve meaningful results aligned with the research objectives. In this study, a two-fold approach was utilized, consisting of both structural analysis and energy evaluation.

## 3.1 STRUCTURAL ANALYSIS OF WIND TOWER

Structural analysis was conducted to determine the compressive forces occurring in the piston rod of the hydraulic cylinder at various positions. These forces were then visually evaluated to identify the optimal position for the specific tower under consideration.

Wind towers are typically manufactured as multiple sections, assembled on-site for easier transportation and installation. However, this also implies non-uniformity in shape throughout the entire height, posing a challenge in accurately determining the weight and center of gravity (COG) for the complete tower.

Each section of the wind tower, including the base, middle, and top sections, is manufactured separately and then connected during the installation process. These sections are often made of steel or other suitable materials, and their dimensions can vary based on the specific design requirements and turbine capacity.

Due to the varying dimensions and shapes of the tower sections, as well as the presence of additional components such as internal platforms, ladders, and equipment rooms, determining the

exact weight and COG of the assembled tower becomes complex. Detailed calculations and engineering analysis are typically required to accurately estimate these parameters. However, for the simplicity of the research in the present study, the wind tower was considered based on the provided specifications, assuming a uniform shape and known weight distribution for the purposes of analysis. Figure 3-1 provides a visual representation of a typical 3D model of the hydraulic erection system.
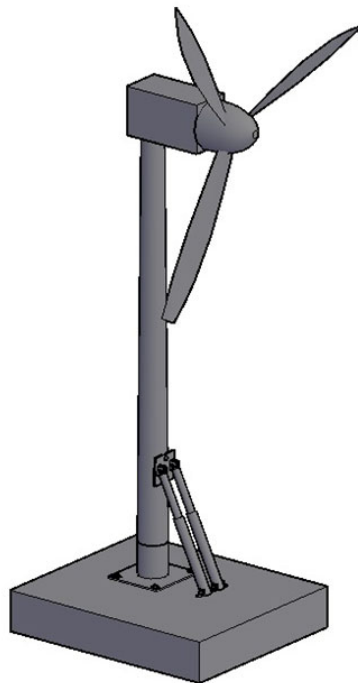


Figure 3-1 Wind tower hydraulic erection system

The tower studied in this research is of small-scale household size, standing at a height of 101 feet. It consisted of a base section with a height of 4 feet, extending from the ground surface to the hinge point. The upper section of the tower measured 97 feet in height. The dimensions of

the tower were selected based on other medium sized wind towers. The base of the tower was cylindrical with a radius of 30.6 inches, while the upper section had a taper ratio of 0.0384 in/in and a top radius of 8.16 inches. The thickness of the tower wall is determined to be 0.311 inches. The wind tower is considered a long linear tapering tower and all other additions such as ladders were neglected. Typical steel with modulus of elasticity 29000 ksi and yield strength 50 ksi was considered as material for the tower build. Figure 3-2 displays a two-dimensional representation of the wind tower, detailing all its parts and dimensions as explained earlier.
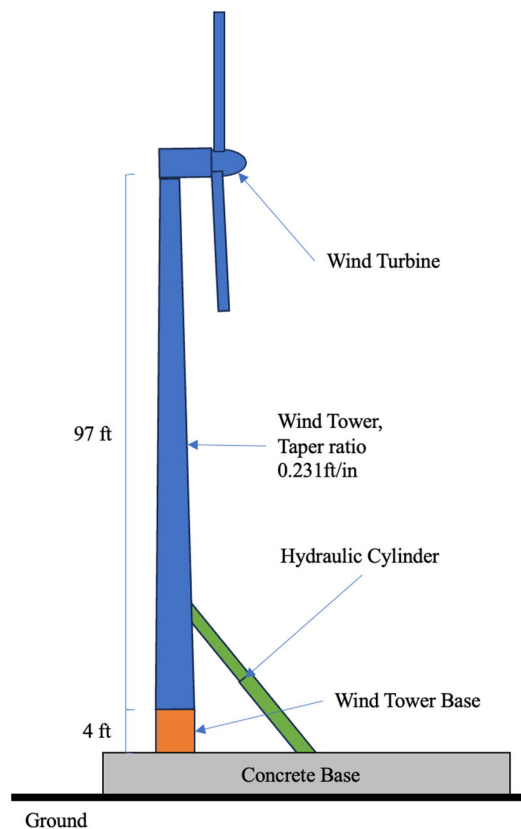


Figure 3-2 Wind turbine tower components and dimensions

To perform the analysis, critical information such as the weight of the entire turbine and its center of mass were required. By varying parameters such as radius, thickness, taper ratio, and height, several alternative versions of the tower were examined.

## 3.2 DETERMINATION OF WIND TURBINE CENTRE OF GRAVITY

The wind turbine considered for the mathematical analysis was based on small scale horizontal axis wind turbines. The wind turbine was divided into different sections, including the blades and hub, generator, and gearbox. The center of gravity of the wind turbine was assumed at 1/3 of its length from the blade for mathematical simplification. Figure 3-3 shows a typical horizontal axis wind turbine and the inner parts.
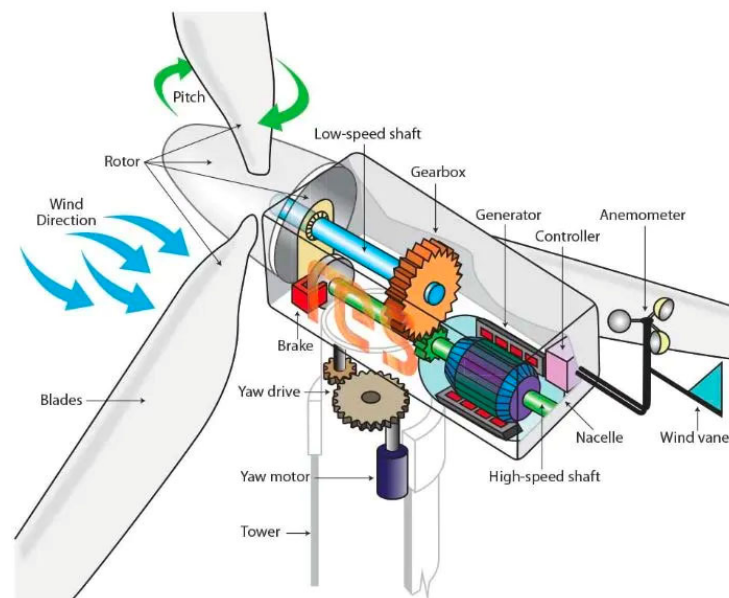


Figure 3-3 Wind turbine parts (WindsmillTech, 2023)

## 3.3 STRUCTURAL ANALYSIS OF WIND TOWER – HYDRAULIC ERECTION SYSTEM

The Structural analysis ascertains the load borne by the hydraulic cylinder during the process of lifting the tower from its resting position to the erect position, as well as returning it to the resting position when required. The assessment of load and stress is accomplished through a

static analysis of the system, considering zero moment at the hinge connection located at the top of the hydraulic tower's base. Figures 3-4 and 3-5 show the 3D model of the hydraulic erection system at an angle with the horizontal and the line diagram of hydraulic erection system at an angle with the horizontal respectively.
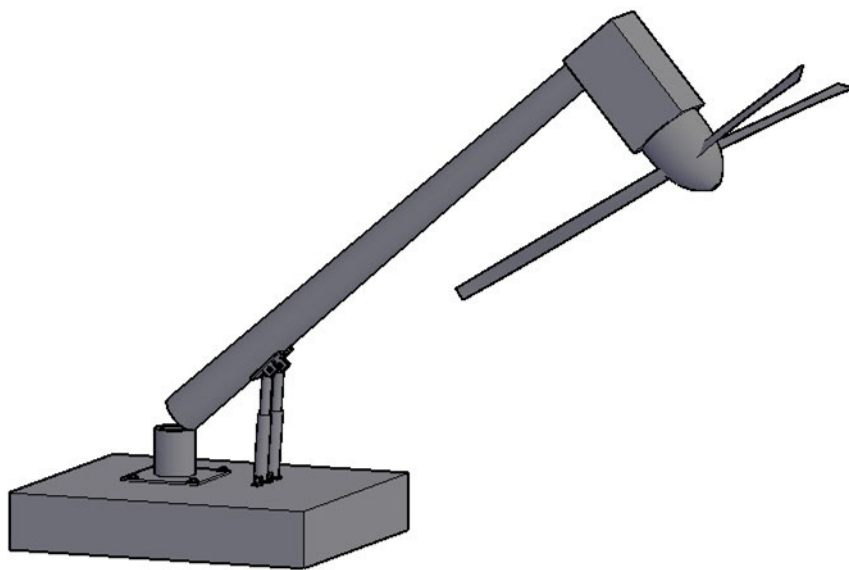


Figure 3-4 3D Model of hydraulic erection system at an angle with horizontal
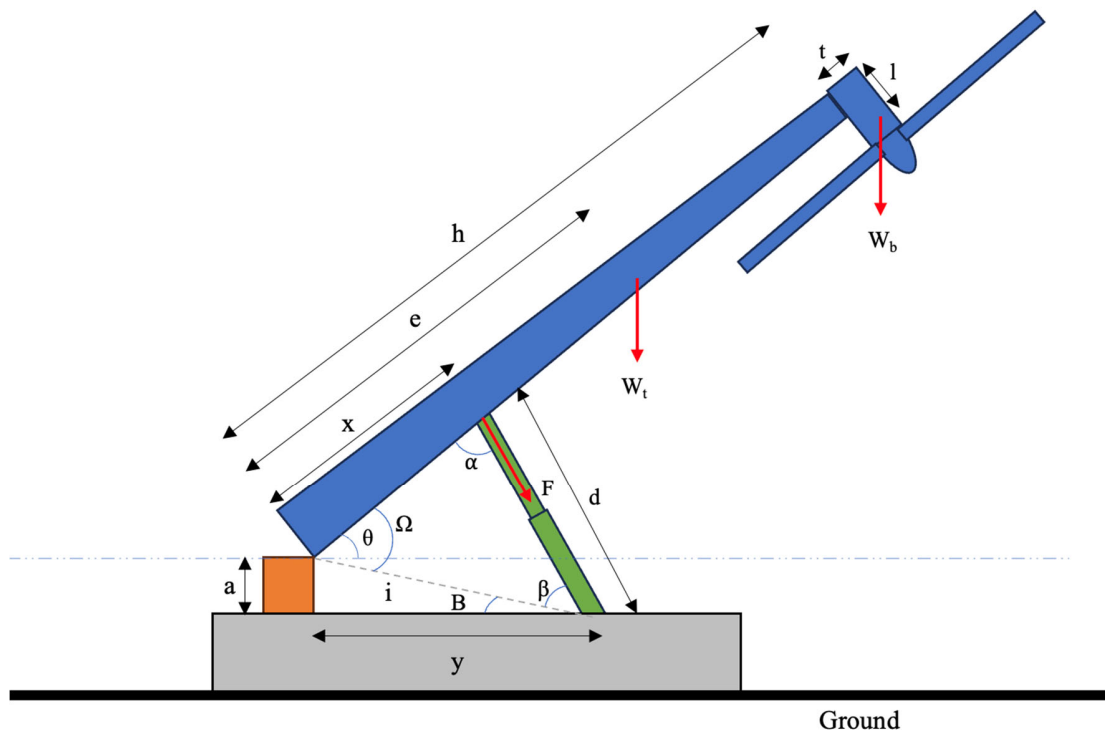
Figure 3-5 Line Diagram of hydraulic erection system at an angle with horizontal

Referring to Figure 3-5, an angle $\theta$ was considered between the wind tower and the horizontal, where the hinge is located. This angle was used to determine the position of the tower with $\theta = 90°$ when the tower is erect while $\theta = 0°$ when the tower is in horizontal position.

The two variable x and y define the connection of the hydraulic cylinder with the wind tower and the ground respectively, where "**y**" is measured from the outer edge of the base and "**x**" is the connection distance from the top of the base to the hydraulic cylinder connection point. "**d**" being the length of the hydraulic cylinder which increases progressively as the tower is raised and subsequently decreases as it is lowered. An imaginary line from the hinge to the base of the

hydraulic cylinder gives two more variables upon which the static analysis of the system is based. "**B**" being the angle of inclination depending upon the base height "**a**" and "**y**".

$$B = \ tan^{-1}\frac{a}{y}$$  (3.1)

The length of the imaginary line is also an important parameter. Although it remains constant throughout the erection or retraction process, it can be used to calculate the length of the hydraulic cylinder throughout the progression. The length "**i**" can be calculated using Pythagoras theorem considering the base is at a 90° with the ground.

$$i = \ \sqrt{a^2 + y^2}$$  (3.2)

$\boldsymbol{\Omega}$ is the angle made by the tower with the imaginary line, it begins from B and reaches the maximum value of 90+B at the erect condition of tower. "$\boldsymbol{\beta}$" is the angle made by the hydraulic cylinder with the imaginary line. Finally, $\boldsymbol{\alpha}$ is the angle made by the hydraulic cylinder with the wind tower. All these angles change as the tower undergoes the process of erection and retraction back to the ground. Thus, they play a part in the force exerted on the hydraulic cylinder in one way or another. The variables, as detailed above, have been compiled in Table 3-1.

Table 3-1 Variables defined in line diagram.

| Legend | |
|---|---|
| x | Connection distance of hydraulic cylinder on wind tower from hinge in ft |
| y | Connection distance of hydraulic cylinder on concrete base from outside surface of base in ft |
| h | Total height of wind tower |
| e | Center of Gravity of Wind Tower from base |
| t | Height of Wind turbine |
| l | Center of Gravity of Wind Tower from edge |
| a | Height of Wind tower base |
| d | Length of Hydraulic Cylinder |
| i | imaginary line connecting top of wind tower base to the base of hydraulic cylinder connected to the concrete base |
| Wt | Total Weight of Wind Tower |
| Wb | Total Weight of Wind Turbine |
| F | Compressive Force on Hydraulic Cylinder |
| θ | Angle made by wind tower with horizontal during erection |
| α | Angle made by hydraulic cylinder with wind tower |
| β | Angle made by imaginary line "i" with hydraulic cylinder |
| B | Angle made by imaginary line "i" with concrete base |
| Ω | Angle made by wind tower with imaginary line "i" during erection |

Using static analysis, the moment about the hinge can be taken as zero and as such the force

required by the hydraulic cylinder can be determined as.

$$\sum Moment\ about\ hinge = 0$$

$$F = -\left(\frac{W_x*e\ cos\ \theta + W_t(l\ sin\ \theta + h\ cos\ \theta)}{x\ sin\ \alpha}\right) \tag{3.3}$$

Where, $W_x$ is the weight of the tower, $W_t$ is the weight of turbine, l is the centroid of turbine, h is the total length of the tower, e is the centroid of tower, x is the length of connection of hydraulic cylinder on tower from hinge and F is the force exerted on the hydraulic cylinder.

With the force on the hydraulic cylinder calculated it becomes a simple task to calculate the reactions at hinge using the formula for equilibrium, with $R_x$ being the horizontal reaction and $R_y$ being the vertical reaction at hinge.

$$\sum F_x = 0$$

$$R_x = F\ cos\ \alpha\ cos\ \theta - F\ sin\ \theta\ sin\ \alpha \tag{3.4}$$

Similarly,

$$\sum F_y = 0$$

$$R_y = W_t + W_x - F\ sin\ \alpha\ cos\ \theta - F\ sin\ \theta\ cos\ \alpha \tag{3.5}$$

"$\alpha$", the angle between the hydraulic cylinder and the wind tower changes as the tower is erected or lowered. This angle affects the reactions and can be obtained by the use of sine and cosine laws.

## 3.4 GOVERNING FORCES FOR HYDRAULIC CYLINDER SELECTION

To determine the limitations of the connection, the impacting load capacity must be determined. It must first be established that the sections of the tower where the cylinder is connected is in fact a hollow circular section. The buckling and shear strength conditions of hollow section are only applicable if the slenderness ratio is less than $\frac{0.45E}{F_y}$ given by Equation 3.6 (American Institute of Steel Construction, 2017),

$$\frac{D}{t} < \frac{0.45E}{F_y} \tag{3.6}$$

Since the taper ratio of the tower was already established as 0.0384 in/in and the thickness "t" = 0.311 in.

$$\frac{D - 0.0384x}{0.311} < \frac{0.45E}{F_y} \tag{3.7}$$

In order to avoid the impact of wind or to ignore it per say on the hydraulic cylinder, the maximum height of connection can be limited to 15 ft from the ground or up to 120 inches from the hinge of the wind tower. Since, wind velocity pressure coefficients remain constant up to 15 ft above ground considering terrain with low lying obstructions. (Hibbeler, 2017)

Considering a preliminary value of x = 120 inches, using Equation 3.6.

$$\frac{D - 0.0385x}{0.311} < \frac{0.45E}{F_y}$$

$$181.825 < 261$$

O.K.

37

The connection of hydraulic cylinder to the tower is dependent on the shear strength capacity and buckling strength of the section where it is connected. The wind tower being a truncated cone, each section is a hollow circle.

The nominal shear strength of a hollow circular section is defined according to limit states of shear yielding and buckling (American Institute of Steel Construction, 2017) is determined as.

$$V_n = \frac{F_{cr} A_g}{2} \tag{3.8}$$

Where, $F_{cr}$ shall be the larger of,

$$F_{cr} = \frac{1.6E}{\sqrt{\frac{L_v}{D}} \times \left(\frac{D}{t}\right)^{\frac{5}{4}}} \tag{3.9}$$

$$F_{cr} = \frac{0.78E}{\left(\frac{D}{t}\right)^{\frac{3}{2}}} \tag{3.10}$$

this value shall not exceed 0.6Fy,

where, $A_g$ is the gross cross-sectional area of member, D is the outside diameter $L_v$ is distance from maximum to zero shear force t is the design wall thickness.

For a hollow circular section, since there is no weaker axis to undergo later torsional buckling and instead the section is governed by local buckling or yielding (whichever is smaller). AISC 15th edition, Chapter F gives us the required information for calculating the local buckling strength and yielding strength of a hollow section, since the section has $\frac{D}{t}$ ratio less than $\frac{0.45E}{Fy}$,

Nominal flexural strength, $M_n$ shall be the lower of

$$M_n = M_p = F_y Z \tag{3.11}$$

Or Local buckling Strength,

$$M_n = \left[\frac{0.021E}{\frac{D}{t}} + F_y\right] * S \qquad (3.12)$$

Where S is the elastic modulus of member cross section.

For sections judged to have slender walls

$$M_n = F_{cr}S \qquad (3.13)$$

Where,

$$F_{cr} = \frac{0.33E}{\frac{D}{t}}$$

$F_{cr}$ is the critical stress. Upon analysis, local buckling strength was considered as the governing moment capacity against buckling. A detailed calculation of the structural analysis, moment diagrams and governing forces for the erection system can be found in Appendix A.

### 3.5 SELECTION CRITERIA FOR HYDRAULIC CYLINDERS

The selection of hydraulic cylinders for the purpose of lifting and lowering a tower requires careful consideration of various criteria. In this particular application, the following factors were taken into account to ensure an optimal choice of hydraulic cylinders.

First, the decision was made to prioritize locally available hydraulic cylinders. This choice was driven by the advantages of easy access to spare parts, maintenance services, and technical support, thereby minimizing potential downtime during operation. As discussed previously all data, dimension, carrying capacity, type, retraction load capacity etc., for cylinders considered in this thesis were locally available inside the United States adhering to all these criteria.

To facilitate the lifting and lowering of the tower, hydraulic cylinders with double-acting capabilities were deemed essential. Double-acting cylinders enable force generation in both directions, allowing for efficient and controlled movement during both the upward and downward motions.

To maintain practicality and stability of the system, the primary objective is the selection of hydraulic cylinders with an appropriate diameter. Given the requirement to attach two cylinders, the diameter size must be carefully considered to avoid an excessive diameter that would hinder the installation. By ensuring that the selected cylinders are of suitable dimensions, a streamlined attachment of the hydraulic cylinder to the wind tower can be maintained. Two cylinders are added to facilitate a stable system. Two cylinders are used since a large amount of load is carried by the system. To avoid usage of custom hydraulic cylinder and still allow locally available hydraulic cylinders to be considered two cylinders must be used.

At any position of attachment, there is only a certain portion of the wind tower available for attachment. The two cylinders must also have a healthy space between them to avoid any friction or contact during the lifting or lowering process, which might cause impact on the load carrying capacity of either.

To optimize the design, the hydraulic cylinders were chosen such that their fully closed (largest capacity) diameter was always carrying the wind tower in its lowered condition. Since the system is likely to induce maximum stress on the hydraulic cylinder during its lowered

condition. So, the fully closed length of the hydraulic cylinder must be equal or less that the space left by the wind tower to the ground.

Furthermore, the load carrying capacity of the hydraulic cylinders is a vital consideration. The determination was made to choose cylinders with a load-carrying capacity of at least 125% of the anticipated load (PowerX International, 2018). This safety margin ensures effective handling of the load by the hydraulic cylinders and the ability to withstand unexpected variations or additional forces during operation.

Lastly, the hydraulic cylinders were required to operate at a minimum efficiency level of 70-80%. By setting a minimum efficiency level of 70-80% (PowerX International, 2018), it ensures that the selected hydraulic cylinders operate at an acceptable level of efficiency, thus maximizing the utilization of input power and minimizing energy waste. This directly contributes to optimizing the overall efficiency of the system.

A standard two phase telescopic hydraulic cylinder was selected for carrying out analysis after determining its local availability. The dimensional constraints were considered before selecting the appropriate hydraulic cylinder.

1. The maximum total length of locally available telescopic hydraulic cylinders was found to be 11-12.55 ft.
2. Total available length when tower is lowered is 5.052 ft.
3. $D_{allowable} = \dfrac{\left[\frac{D-0.0384x}{2.5}-2.5\right]}{2.5}$ is the allowable diameter for the hydraulic cylinder as discussed earlier.

Using the above conditions, a locally available hydraulic cylinder for 3000 psi standard.

Strength, 9x8.25x6.75-inch dimension with total length of 12.55 ft was selected. The following

equations were then generated based on the static analysis carried out earlier to find a range of

values where the cylinder could be connected.

Considering the tower is fully erect,

$$(x + 4)^2 + y^2 \leq d^2 \tag{3.14}$$

Considering the tower is in the fully lowered position, the controlling equation considers the

largest section of the cylinder as responsible for carrying the wind tower in its fully lowered

state.

Using the Cosine law in the triangle, Equation 3.14 can be formulated when the hydraulic

cylinder is at a fully lowered condition.

$$\sqrt{x^2 + \sqrt{(4^2 + y^2)}^2 - 2 \times x \times \sqrt{(4^2 + y^2)} \, cos(tan^{-1}\frac{4}{y})} \leq$$

$retracted\ space\ when\ fully\ lowered$ (3.15)

Figure 3-6 displays the hydraulic erection system at fully lowered condition representing the

retracted space in Equation 3.15.
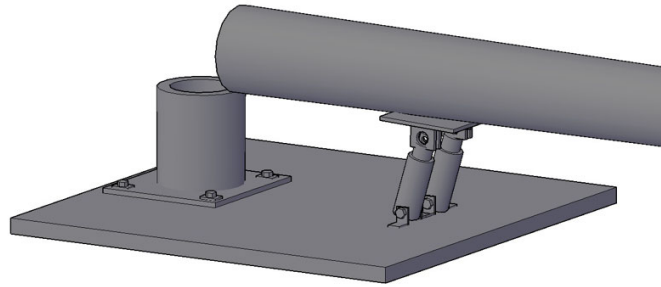
Figure 3-6 Hydraulic erection system in fully lowered condition

These equations were used to plot a graph and identify applicable feasible values for the hydraulic cylinder connection. The graph in Figure 3-7 illustrates the satisfactory region, taking into account the dimensional limitations. The red circle represents Equation 3.14, and the blue triangular section represents Equation 3.15. the intersection of these equations also considering that both x and y need to be greater than zero, gives us the satisfactory region of values highlighted in green.
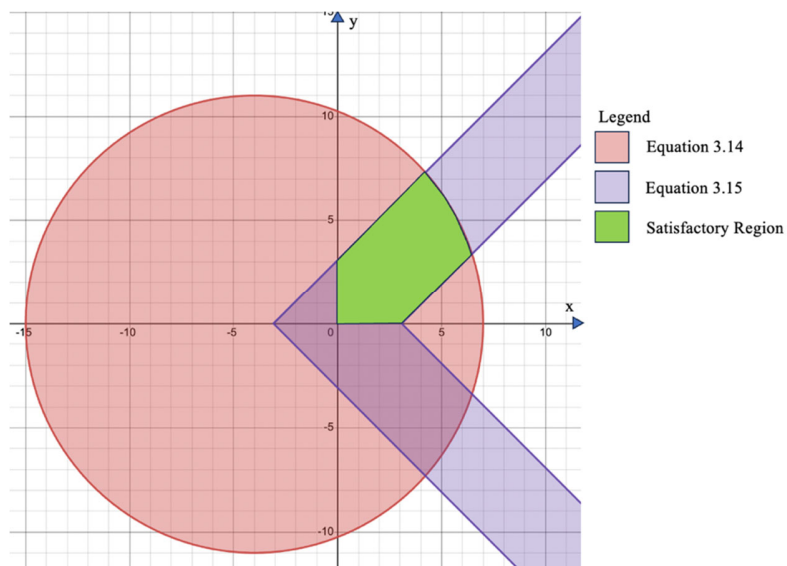


Figure 3-7 Dimensional limitations for hydraulic cylinder selection

Based on the feasible region a set of points was collected which were the applicable values for both x and y. It was assumed that the connections can be made at an interval of six inches only. So, the value of x ranges from 7.5 ft to 1ft from the base of the wind tower. Equation 3.15 shows the range of applicable values for y.

$$y = x \pm 3.033 \tag{3.15}$$

Such that the values do not exceed 8.378 ft and are not less than 3.033 ft and the total length does not exceed the allotted amount.

## 3.6 ENERGY CONSUMPTION CALCULATION

### 3.6.1 PROTOTYPE ANALYSIS

To study the actual energy consumed by the hydraulic erection system on field a prototype was prepared. The construction of the erection system prototype followed a simple design comprising key components. The primary structure consisted of a hollow steel cylinder with a diameter of 12 inches. The cylinder featured a hinge located approximately 1/4th of the way from the bottom, enabling the tower section to be raised and lowered using a hydraulic pump, while the base section remained fixed in position. To prevent undesired movement, the base was securely fastened to a wooden board.

The hydraulic pump was positioned on a longer wooden board, which included a metal track on top. The bottom of the pump shaft was equipped with rollers that ran along this track, allowing for adjustment of the pump's location by sliding it back and forth. This adjustment capability facilitated changes in the stroke angle.

The top of the pump shaft was attached to a metal plank with holes, offering further adjustability by modifying the position of this board, which was in turn connected to the tower. This arrangement provided flexibility in controlling the height of the pump and its corresponding impact on the tower.

As for the representation of the wind turbine blades, a 45-lb barbell plate was strapped to the top of the tower. Additional support was provided by a horizontally attached pole, situated 3 and 1/8 inches from the top of the tower, to secure the plate in place. Figure 3-8 shows the protype erection system along with all its parts assembled for energy consumption tests.
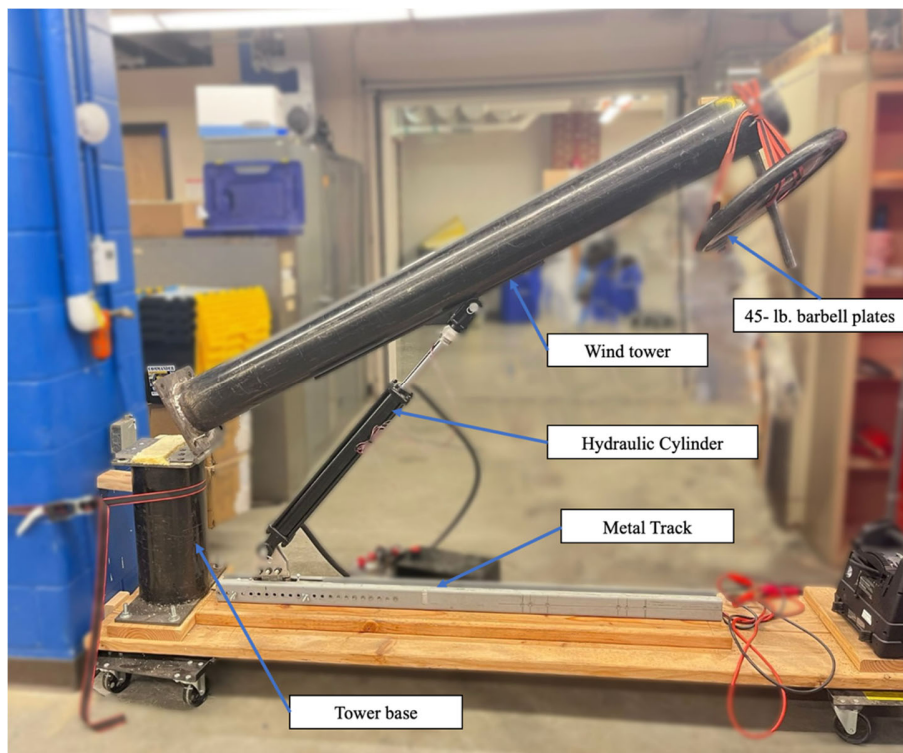


Figure 3-8 Prototype hydraulic erection system.

To carry out the test to determine the most energy efficient position of the hydraulic cylinder, three different distances between the base of the pump shaft and the cylinder base were tested: 11 in., 9 in., and 9.5 in. To quantify energy consumption, a current meter was connected to the pump's power supply wire, and the initial and final voltages of the battery were recorded.

During test trials, the current, time, and cylinder angle were recorded at each position during the raising and lowering operations. This data allowed for the calculation of the energy consumed by the pump at different angles. The experimental energy consumption was then compared to the theoretical energy required to raise the wind turbine. In Figure 3-9, a portrayal of the prototype hydraulic cylinder's erection at various angles can be observed.



(a)                                           (b)

(c)                                        (d)
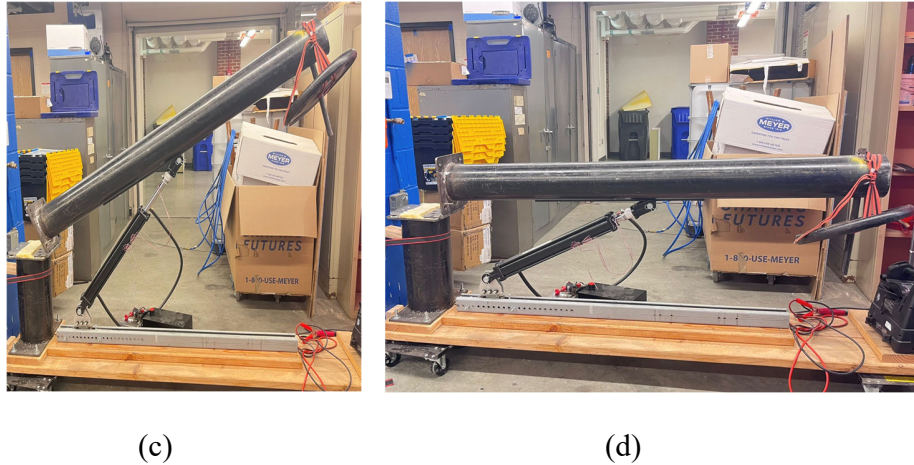
Figure 3-9 Prototype erection system at different angles a) 75° b) 45° c) 30° d) 0°

The theoretical energy calculations were based on the gravitational potential energy equation, considering the mass of the wind turbine and the height change during the raising process. By assuming a static state, the required theoretical energy was determined for each angle. This process was repeated for all three pump positions, and four trials were conducted for each position. Two trials started from the bottom position, while the other two started from the top position, ensuring comprehensive analysis of energy efficiency across different starting points. Industrial formulas pertaining to the hydraulic cylinder used were also used to calculate the energy produced and all three results were compared. Table 3-2 below presents data related to the hydraulic cylinder utilized in the prototype wind tower.

Table 3-2 Properties of hydraulic cylinder used for prototype wind tower.

| Hydraulic Cylinder Properties | |
|---|---|
| Cylinder Type | Tie Rod |
| Action | Double- Acting |
| Bore (ID) | 2.5" |
| Stroke | 20" |
| Rod (OD) | 1.125" |

| | |
|---|---|
| Mounting Type | Clevis |
| Mounting Pin (OD) | 1" |
| Rod End Type | Clevis |
| Rod End Pin (OD) | 1" |
| Work Ports | 3/8" NPT(F) |
| Max Working Pressure | 3000 psi |
| Retracted Length | 30.25" (pin to pin, center to center) |
| Extended Length | 50.25" (pin to pin, center to center) |
| Cylinder Length | 32.26" (retracted, edge to edge) |
| Product Weight | 31.00 lbs |

### 3.6.2 ENERGY CONSUMPTION BY WIND TOWER ERECTION SYSTEM

Field investigation would be required to calculate the energy consumption by the actual

hydraulic erection system. Since that was no possible, the prototype was taken as a reference,

and it was assumed that the actual wind tower erection system would follow the electrical energy

consumption trend of the prototype. To further validate this, industrial formulas obtained from

manufacturers and the maximum load carried were used to calculate the horsepower utilized by

the system. Equation 3.16 (Aggressive Hydraulics, 2019 and Flodraulic, 2019)

shows the fluid horsepower of a hydraulic cylinder based on pressure produced.

$$Fluid\ Power\ Horsepower(HP) = \frac{(Pressure\ (psi)\ \times\ pump\ flow\ (gpm))}{1,714} \tag{3.16}$$

A detailed calculation of energy consumption by prototype and the wind erection system can be

found in Appendix B.

# CHAPTER 4: **RESULTS**

This chapter encompasses the results of the thesis. The range of values calculated in the methodology were used as the position of the hydraulic cylinder. Each combination of values was tested to find the position that yielded the least amount of compressive force on the hydraulic cylinder. The following sections show the results of the analysis. The range of data used for this analysis is presented in Figure 4-1. The variables outlined in Figure 4-2 and Table 4-1 will serve as the basis for explaining the results in this section.
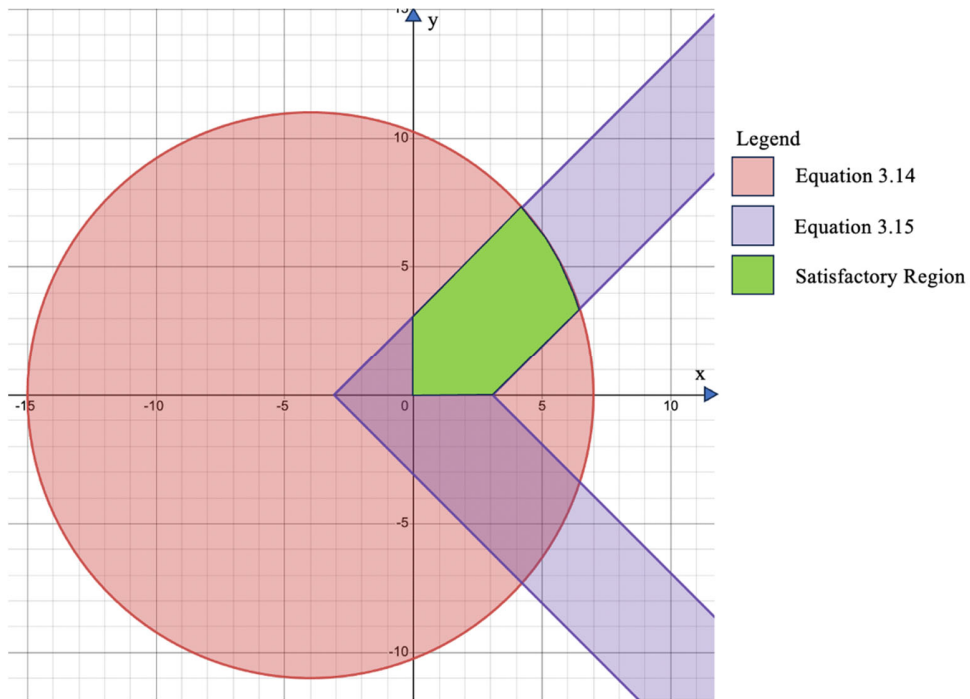


Figure 4-1 Dimensional limitations for hydraulic cylinder selection
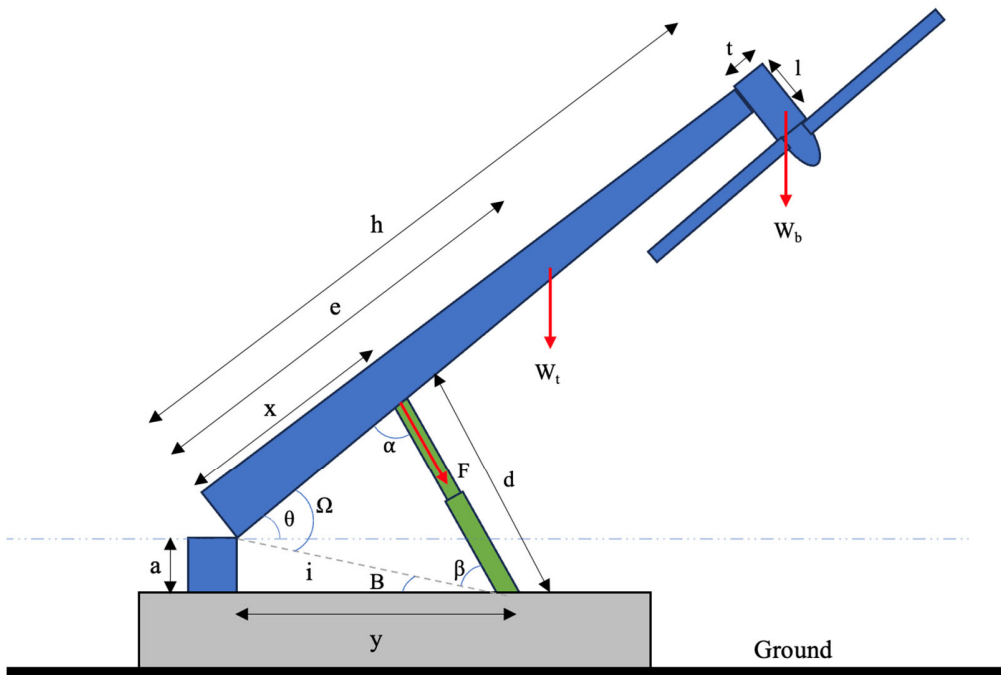
Figure 4-2 Line Diagram of hydraulic erection system at an angle with horizontal

Table 4-1 Variables defined in line diagram.

| | Legend |
|---|---|
| x | Connection distance of hydraulic cylinder on wind tower from hinge in ft |
| y | Connection distance of hydraulic cylinder on concrete base from outside surface of base in ft |
| h | Total height of wind tower |
| e | Center of gravity of wind tower from base |
| t | Height of wind turbine |
| l | Center of gravity of wind tower from edge |
| a | Height of wind tower base |
| d | Length of hydraulic cylinder |
| i | imaginary line connecting top of wind tower base to the base of hydraulic cylinder connected to the concrete base |
| Wt | Total weight of wind tower |
| Wb | Total weight of wind turbine |
| F | Compressive force on hydraulic cylinder |
| θ | Angle made by wind tower with horizontal during erection |
| α | Angle made by hydraulic cylinder with wind tower |
| β | Angle made by imaginary line "i" with hydraulic cylinder |
| B | Angle made by imaginary line "i" with concrete base |
| Ω | Angle made by wind tower with imaginary line "i" during erection |

## 4.1 RELATIONSHIP BETWEEN θ AND COMPRESSIVE FORCE ON CYLINDER

The changes in hydraulic cylinder force are graphically represented in Figure 4-3, corresponding to the wind tower's inclination angle, ranging from 0° (lowered) to 90° (erect) condition. Results for four different positions have been presented in the figure with different connection details, where $\alpha_i$ is the initial angle, the hydraulic cylinder makes with the wind tower at $\theta = 90°$.
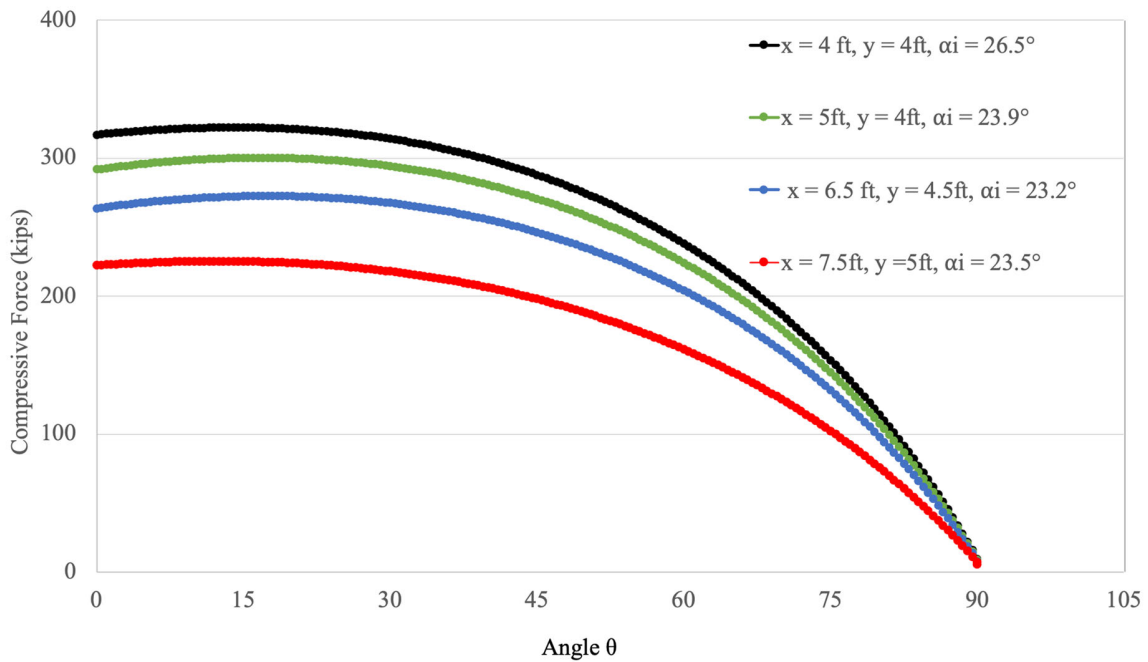


Figure 4-3 Compressive force vs Angle θ at various connection locations

At $\theta = 0°$ when the tower is fully lowered, the hydraulic cylinder carries almost all the weight of the tower as well as balancing the moment produced due to the weight of the tower and the wind turbine. As the tower is raised and the angle θ increases, the weight and moment are shared with the hinge, the force is transferred to the base and finally to the ground. When the tower is fully erected, almost all the weight is transferred to the ground, although the hydraulic cylinder still carries some force generated by the moment caused by the wind turbines. Equation 4.1 represents the compressive force on the hydraulic cylinder.

52

$$F = -\frac{W_t \times e\cos\theta + W_b \times (h\cos\theta + l\sin\theta)}{x \times \sin\alpha} \qquad (4.1)$$

Referring to this equation, the compressive force is dependent upon the moment created by the turbine and the wind tower itself. The maximum value for both these moments combined can be seen when the tower reaches 15°-20°.

## 4.2 RELATIONSHIP BETWEEN θ AND REACTION AT HINGE

As the tower is raised, there is an upward reaction at the hinge, which needs to be balanced by adding appropriate bolts. This upward force is caused by the hydraulic cylinder force and the moment of the entire system trying to push the wind tower towards the gravity direction. Equation 4.2 represents the equation for vertical reaction as the tower is lowered or erected.

$$R_y = W_t + W_b - F \times \cos\alpha \times \sin\theta - F \times \sin\alpha \times \cos\theta \qquad (4.2)$$

The vertical reaction is dependent upon the angle α, the angle between the wind turbine tower and the connection of hydraulic cylinder at the wind tower. As the tower is erected, up to θ = 20°, the horizontal and vertical component of the compressive force is maximum. As shown by Figure 4-3 up to 20° the compressive strength has an increasing trend. As the tower is raised, more and more load is carried by the hydraulic cylinder which eventually reaches a minimum as the entire weight is now carried by the ground/ hinge reaction. The following Figure 4-4 shows the relationship between the vertical reaction at hinge and angle θ at various positions.
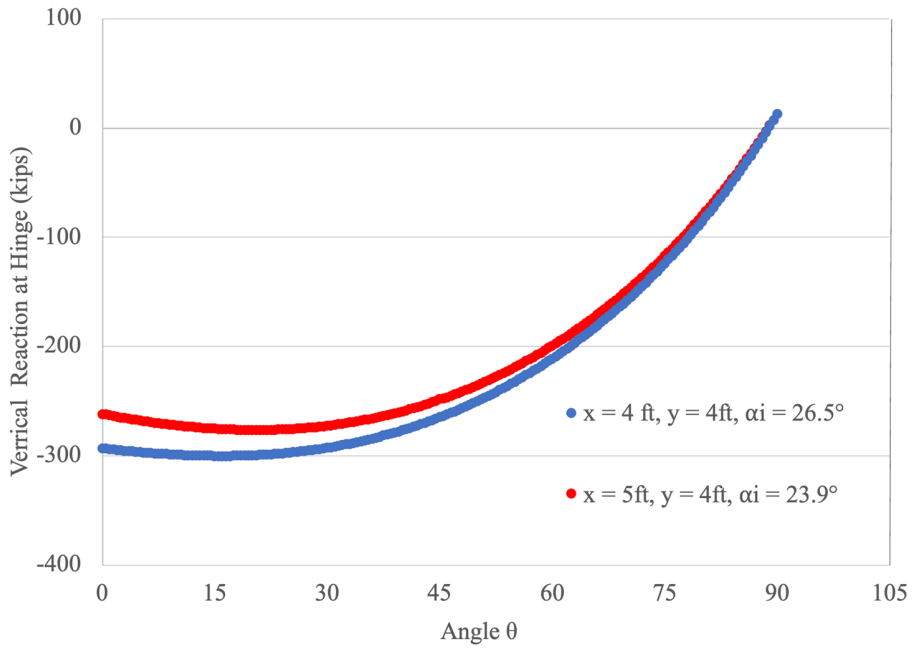
Figure 4-4 Vertical reaction at hinge Vs Angle θ at various connection location.

Figure 4-5 provides a graphical presentation of how the reaction at the hinge increases and the force at the cylinder decreases when the tower is raised from its initial lowered state when x = 7.5 ft and y = 5ft.
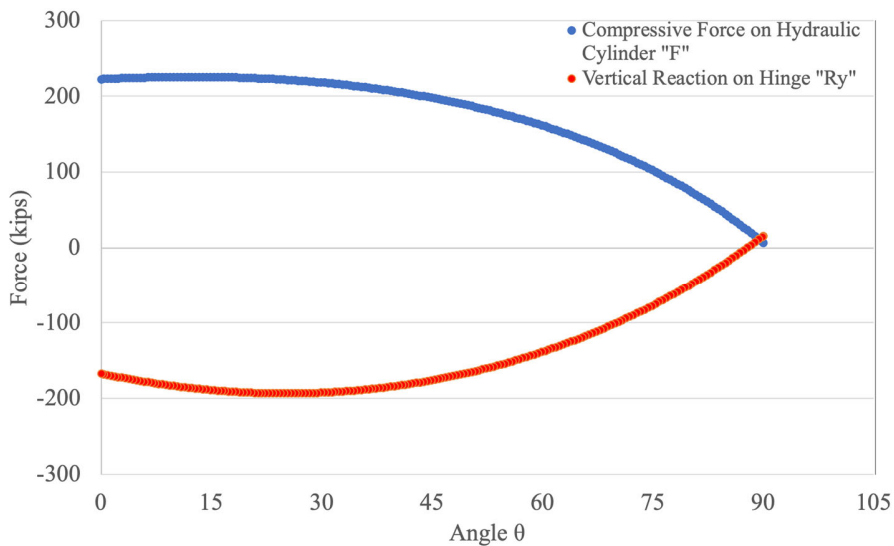


Figure 4-5 Compressive force on cylinder vs vertical reaction at hinge.

## 4.2.1 RELATIONSHIP BETWEEN θ AND HORIZONTAL REACTION AT HINGE

As the tower is raised from its lowered position, the horizontal force keeps on decreasing as more and more load is being transferred to the ground via the hinge. The Equation 4.3 represents the equation for horizontal reaction as the tower is lowered or erected.

$$R_x = F \times sin\alpha \times sin\theta - F \times cos\alpha \times cos\theta \qquad (4.3)$$

The horizontal reaction is dependent upon the angle α, the angle between the wind turbine tower and the connection of hydraulic cylinder at the wind tower itself. As the tower is erected this angle decreases, and increases when the tower is erected. Between θ = 15° - 39°, the tower is at horizontal equilibrium and then as the angle increases the force changes direction and subsequently comes back down. At 90°, most of the weight is directly transferred to the ground and only a small amount of reaction can be seen due to the moment produced by the wind turbine. The relationship between the horizontal reaction and the angle θ is displayed in Figure 4-6.
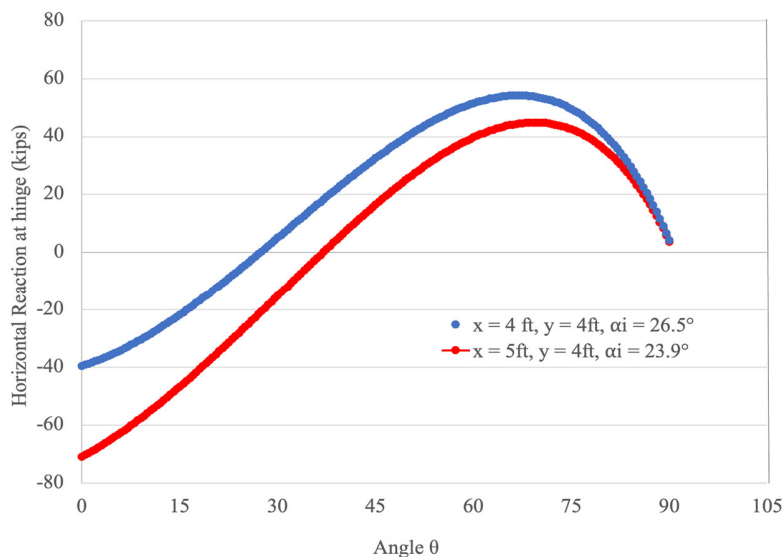


Figure 4-6 Horizontal reaction at hinge Vs Angle θ at various connection location.

Figure 4-7 shows a graph representing the relationship between the horizontal reaction and compressive force on the hydraulic cylinder as the tower is raised from its lowered position. Here the connection details are as follows: x = 7.5ft, y = 5ft.
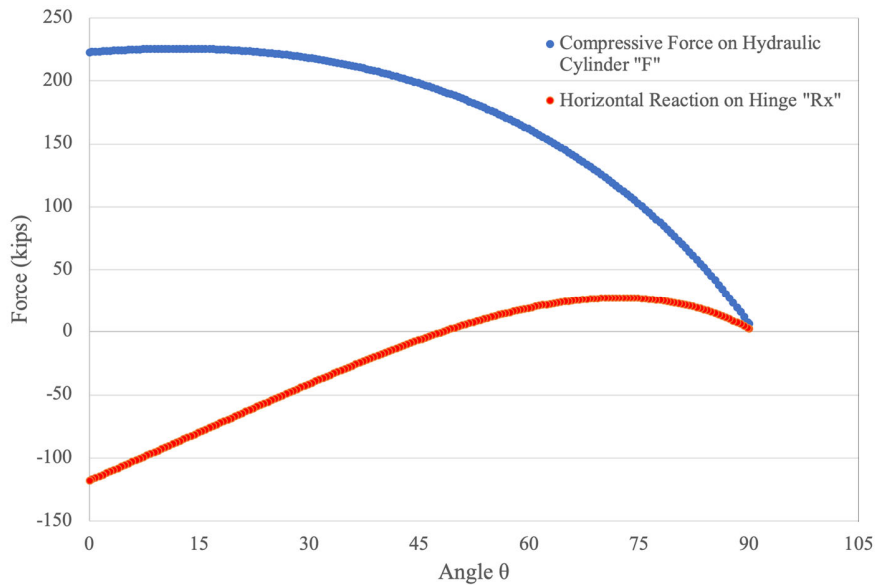


Figure 4-7 Compressive force on cylinder vs horizontal reaction at hinge.

### 4.3 COMPRESSIVE FORCE AT VARIOUS ANGLES

As the connection at base is further and further away from the base, the reaction on the cylinder continues to show a decrease. The value reaches a minimum when the connection at base and the connection at wind tower is roughly the same. (7.5ft each in this case) beyond this, the value of force on hydraulic cylinder once again increases gradually contrary to before. The following Table 4-2 presents the variations in hydraulic cylinder force while the connection at the wind tower's "x" is maintained at a constant value.

Table 4-2 Force on hydraulic cylinder varying connection at wind tower "x" constant

| No. | Connection at Wind tower "x" (ft) | Connection at concrete base "y" (ft) | Maximum Force on Cylinder (kips) |
|---|---|---|---|
| 1 | 7.5 | 1 | 396.1 |
| 2 | 7.5 | 2 | 332.5 |
| 3 | 7.5 | 3 | 288.1 |
| 4 | 7.5 | 4 | 253.2 |
| 5 | 7.5 | 5 | 225.6 |
| 6 | 7.5 | 6 | 205.3 |
| 7 | 7.5 | 7 | 192.3 |
| 8 | 7.5 | 7.5 | 188.9 |
| 9 | 7.5 | 8 | 190.4 |
| 10 | 7.5 | 9 | 202.7 |
| 11 | 7.5 | 10 | 224.1 |
| 12 | 7.5 | 11 | 254.6 |

At steeper angles, (connection at base father away from the connection at wind tower) the hydraulic cylinder not only has to overcome the weight of the wind tower, but also the moment that is generated on itself. When both values are equal and the hydraulic cylinder is vertical, the moment generated is the lowest and hence, the force produced as well. In general condition, where there are no dimensional restraints, this condition can be considered the most effective or optimal position for the placement of hydraulic cylinder.

Figure 4-8 illustrates how the force changes when the connection of the hydraulic cylinder is moved in relation to the concrete base.
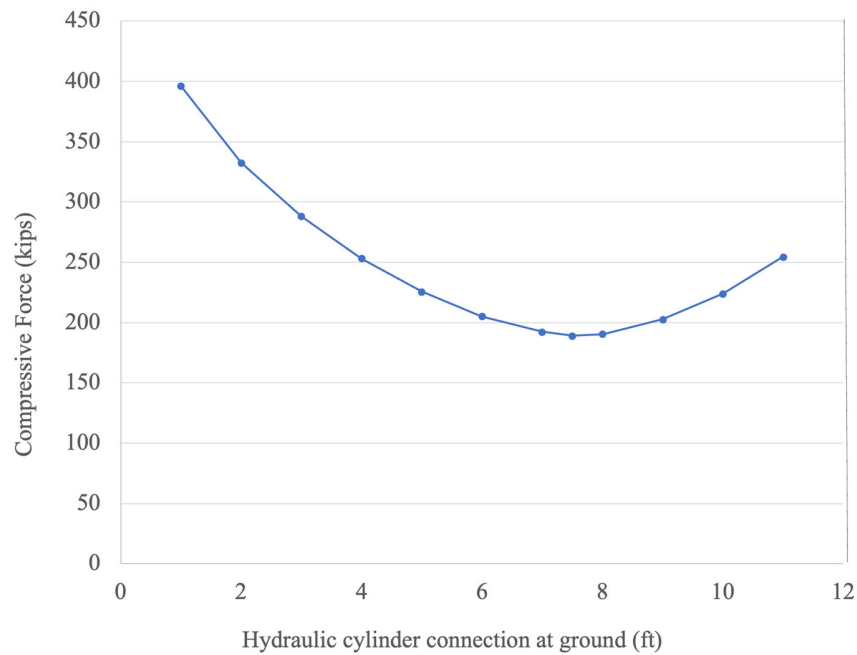
Figure 4-8 Compressive force on hydraulic cylinder vs connection at base.

In this case, the values of both 7.5 ft on base and wind tower, unfortunately, cannot be created. Since available space for hydraulic cylinder connection is very small and the large bore or cylinder needed to be in connection when the wind tower was at its lowered position.

As the connection at the wind tower goes on increasing the reaction on the cylinder decreases, significantly at first and then at a very minor rate. The value continues to decrease the higher the connection is made. Unless the connections are made at a significantly larger height, it can be seen that there is no major change in the load induced that may heavily impact the hydraulic cylinder. The table 4-3 shows how the force of the hydraulic cylinder changes when the connection of hydraulic cylinder with the ground "y" is kept constant.

Table 4-3 Force on hydraulic cylinder varying connection at wind tower "x".

| No. | Connection at Wind tower "x" (ft) | Connection at concrete base "y" (ft) | Maximum Force on Cylinder (kips) |
|---|---|---|---|
| 1 | 1 | 5 | 2009.4 |
| 2 | 2 | 5 | 887.6 |
| 3 | 3 | 5 | 528.8 |
| 4 | 4 | 5 | 365.3 |
| 5 | 5 | 5 | 283.5 |
| 6 | 6 | 5 | 248.9 |
| 7 | 7 | 5 | 230.9 |
| 8 | 7.5 | 5 | 225.6 |
| 9 | 8 | 5 | 222.2 |
| 10 | 9 | 5 | 220.2 |
| 11 | 10 | 5 | 217.2 |
| 12 | 11 | 5 | 213.6 |

Selection of hydraulic cylinder is made easier by this data. Beyond 7.5 ft there is no significant load impact on the hydraulic cylinder. While connections at significantly higher position may drastically reduce the load impact, economic restraints, transportation and maintenance issues and unfeasible cylinder design, however, are what makes the connection at a significantly higher level unviable. Figure 4-9 illustrates a graph representing the force generated while moving the connection of the hydraulic cylinder with the wind turbine tower.
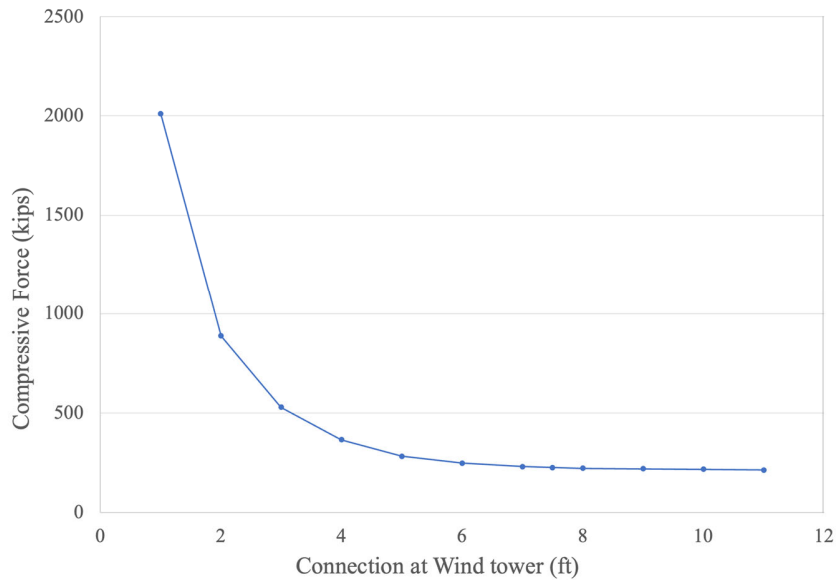
Figure 4-9 Compressive force on hydraulic cylinder vs connection at wind tower

Considering these two results, x = 7.5ft and y = 7.5ft is the connection point that yield the lowest force on the hydraulic cylinder. However, due to the dimensional constraints of the hydraulic cylinder such a connection is not possible. Hence. The next best possible connection point would be x= 7.5ft and y = 5ft.

## 4.4 HYDRAULIC CYLINDER CAPACITY

The following tables shows the comparison between two applicable positions for the hydraulic cylinder based on the range calculated earlier. Here d is the total length of the hydraulic cylinder, F is the compressive force produced in the hydraulic cylinder, Capacity represents the amount of force the cylinder is rated to carry with that particular section and the final column PASS checks whether the cylinder capacity is greater than or equal to the force produced on the cylinder, PASS means the cylinder is able to carry the force and FAIL means that the cylinder cannot produce the required amount of force. Tables 4-4 and 4-5 provide a comparison as the wind turbine tower is elevated from its lowered state to the erect position, while Tables 4-6 and 4-7

offer a comparison as the wind turbine tower is lowered from its erect position to the lowered state.

Table 4-4 Cylinder capacity check (x= 3.5 ft y= 5 ft and x= 4.5 ft, y= 5 ft), Tower Erection

| θ | x= 3.5 ft, y = 5ft | | | | x = 4.5 ft, y = 5 ft | | | |
|---|---|---|---|---|---|---|---|---|
| | d (ft) | F (kips) | Capacity (kips) | PASS | d (ft) | F (kips) | Capacity (kips) | PASS |
| 90.0 | 9.0 | 9.8 | 320.7 | PASS | 9.9 | 8.3 | 320.7 | PASS |
| 80.8 | 8.7 | 108.7 | 320.7 | PASS | 9.5 | 92.2 | 320.7 | PASS |
| 70.8 | 8.3 | 188.8 | 320.7 | PASS | 9.0 | 159.5 | 320.7 | PASS |
| 60.8 | 7.8 | 249.0 | 320.7 | PASS | 8.4 | 209.2 | 320.7 | PASS |
| 50.8 | 7.3 | 295.0 | 320.7 | PASS | 7.8 | 245.9 | 320.7 | PASS |
| 40.8 | 6.7 | 330.3 | 448.0 | PASS | 7.1 | 272.6 | 448.0 | PASS |
| 30.8 | 6.1 | 357.9 | 448.0 | PASS | 6.4 | 291.1 | 448.0 | PASS |
| 20.8 | 5.5 | 380.5 | 448.0 | PASS | 5.7 | 303.2 | 448.0 | PASS |
| 14.8 | 5.2 | 393.3 | 448.0 | PASS | 5.2 | 308.1 | 448.0 | PASS |
| 10.8 | 4.9 | 402.1 | 448.0 | PASS | 4.9 | 310.7 | 448.0 | PASS |
| 0 | 4.3 | 432.2 | 448.0 | PASS | 4.0 | 317.2 | 448.0 | PASS |

Table 4-5 Cylinder capacity check (x= 6.5 ft y= 5 ft and x= 7.5 ft, y= 5 ft), Tower Erection

| θ | x = 6.5 ft, y = 5 ft | | | | x = 7.5 ft y = 5 ft | | | |
|---|---|---|---|---|---|---|---|---|
| | d (ft) | F (kips) | Capacity (kips) | PASS | d (ft) | F (kips) | Capacity (kips) | PASS |
| 90.0 | 11.2 | 7.1 | 320.7 | PASS | 12.5 | 6.3 | 320.7 | PASS |
| 80.8 | 10.7 | 78.3 | 320.7 | PASS | 12.0 | 70.2 | 320.7 | PASS |
| 70.8 | 10.1 | 135.1 | 320.7 | PASS | 11.4 | 121.3 | 320.7 | PASS |
| 60.8 | 9.5 | 176.6 | 320.7 | PASS | 10.6 | 158.7 | 320.7 | PASS |
| 50.8 | 8.7 | 206.8 | 320.7 | PASS | 9.8 | 185.9 | 320.7 | PASS |
| 40.8 | 7.9 | 227.8 | 320.7 | PASS | 8.9 | 205.0 | 320.7 | PASS |
| 30.8 | 7.1 | 241.1 | 320.7 | PASS | 8.0 | 217.4 | 320.7 | PASS |
| 20.8 | 6.2 | 247.8 | 448.0 | PASS | 7.0 | 223.9 | 320.7 | PASS |
| 14.8 | 5.6 | 248.9 | 448.0 | PASS | 6.3 | 225.5 | 448.0 | PASS |
| 10.8 | 5.2 | 248.5 | 448.0 | PASS | 5.9 | 225.5 | 448.0 | PASS |
| 0 | 4.1 | 243.3 | 448.0 | PASS | 4.7 | 222.7 | 448.0 | PASS |

Above is the comparison between two applicable positions for the hydraulic cylinder based on the range calculated earlier. While the tower is being erected, the force provided by the cylinder is enough to carry out the erection when placed at the optimal position. The following tables show, how during the retraction process, the locally available hydraulic cylinder selected is unable to produce enough force capacity to bring the tower back to the ground without failure.

Table 4-6 Cylinder capacity check (x= 3.5 ft y= 5 ft and x= 4.5 ft, y= 5 ft), Tower Retraction

| θ | x= 3.5 ft, y = 5 ft | | | | x = 4.5 ft, y = 5 ft | | | |
|---|---|---|---|---|---|---|---|---|
| | d (ft) | F (kips) | Capacity (kips) | PASS | d (ft) | F (kips) | Capacity (kips) | PASS |
| 90.0 | 9.0 | 9.8 | 106.0 | PASS | 9.9 | 8.3 | 106.0 | PASS |
| 80.3 | 8.7 | 113.3 | 106.0 | FAIL | 9.4 | 96.1 | 106.0 | PASS |
| 70.8 | 8.3 | 188.8 | 106.0 | FAIL | 9.0 | 159.5 | 106.0 | FAIL |
| 60.8 | 7.8 | 249.0 | 106.0 | FAIL | 8.4 | 209.2 | 106.0 | FAIL |
| 50.3 | 7.2 | 297.0 | 106.0 | FAIL | 7.8 | 247.5 | 106.0 | FAIL |
| 40.3 | 6.7 | 331.8 | 127.2 | FAIL | 7.1 | 273.7 | 127.2 | FAIL |
| 30.8 | 6.1 | 357.9 | 127.2 | FAIL | 6.4 | 291.1 | 127.2 | FAIL |
| 20.3 | 5.5 | 381.6 | 127.2 | FAIL | 5.6 | 303.6 | 127.2 | FAIL |
| 14.8 | 5.2 | 393.3 | 127.2 | FAIL | 5.2 | 308.1 | 127.2 | FAIL |
| 10.3 | 4.9 | 403.3 | 127.2 | FAIL | 4.8 | 311.0 | 127.2 | FAIL |
| 0.0 | 4.3 | 432.2 | 127.2 | FAIL | 4.0 | 317.2 | 127.2 | FAIL |

Table 4-7 Cylinder capacity check (x= 6.5 ft y= 5 ft and x= 7.5 ft, y= 5 ft), Tower Retraction

| θ | x = 6.5 ft, y = 5 ft | | | | x = 7.5 ft y = 5 ft | | | |
|---|---|---|---|---|---|---|---|---|
| | d (ft) | F (kips) | Capacity (kips) | PASS | d (ft) | F (kips) | Capacity (kips) | PASS |
| 90.0 | 11.2 | 7.1 | 106.0 | PASS | 12.5 | 6.3 | 106.0 | PASS |
| 80.3 | 10.7 | 81.6 | 106.0 | PASS | 12.0 | 73.2 | 106.0 | PASS |
| 70.8 | 10.1 | 135.1 | 106.0 | FAIL | 11.4 | 121.3 | 106.0 | FAIL |
| 60.8 | 9.5 | 176.6 | 106.0 | FAIL | 10.6 | 158.7 | 106.0 | FAIL |
| 50.3 | 8.7 | 208.0 | 106.0 | FAIL | 9.8 | 187.0 | 106.0 | FAIL |
| 40.3 | 7.9 | 228.6 | 127.2 | FAIL | 8.9 | 205.8 | 127.2 | FAIL |
| 30.8 | 7.1 | 241.1 | 127.2 | FAIL | 8.0 | 217.4 | 127.2 | FAIL |
| 20.3 | 6.1 | 248.0 | 127.2 | FAIL | 6.9 | 224.1 | 127.2 | FAIL |
| 14.8 | 5.6 | 248.9 | 127.2 | FAIL | 6.3 | 225.5 | 127.2 | FAIL |
| 10.3 | 5.2 | 248.4 | 127.2 | FAIL | 5.9 | 225.5 | 127.2 | FAIL |
| 0.0 | 4.1 | 243.3 | 127.2 | FAIL | 4.7 | 222.7 | 127.2 | FAIL |

### 4.4.1 CUSTOM HYDRAULIC CYLINDER

All issues faced by the locally available hydraulic cylinders are cleared by the use of custom cylinders. Since these cylinders are designed specifically to tackle the issues at hand, they are capable of having enough strength to safely operate the wind tower system. The tower can be safely erected and lowered. Further research is required to see the full economic implications of designing a custom hydraulic cylinder of the calculated specifications.

The following tables shows the comparison between two applicable positions for a custom Hydraulic cylinder designed based on the short comings of the local hydraulic cylinder. Here the final column PASS checks whether the cylinder capacity is greater than or equal to the force produced on the cylinder, PASS means the cylinder is able to carry the force and FAIL means the cylinder cannot produce the required amount of force.

Table 4-8 Custom cylinder capacity check, Tower Erection.

| θ | Carrying Section (in) | x= 7.5 ft y = 5 ft | | | x= 4 ft, y = 4.5 ft | | |
|---|---|---|---|---|---|---|---|
| | | Force on Cylinder (kips) | Cylinder Capacity (kips) | PASS | Force on Cylinder (kips) | Cylinder Capacity (kips) | PASS |
| 90 | 9.75 | 6.343 | 416 | PASS | 8.3 | 416 | PASS |
| 80 | 9.75 | 70.245 | 416 | PASS | 92.2 | 416 | PASS |
| 70 | 9.75 | 121.279 | 416 | PASS | 159.5 | 416 | PASS |
| 60 | 9.75 | 158.683 | 416 | PASS | 209.2 | 416 | PASS |
| 50 | 9.75 | 185.898 | 416 | PASS | 245.9 | 416 | PASS |
| 40 | 9.75 | 205.006 | 416 | PASS | 272.6 | 416 | PASS |
| 30 | 9.75 | 217.363 | 416 | PASS | 291.1 | 416 | PASS |
| 20 | 9.75 | 223.940 | 416 | PASS | 303.2 | 416 | PASS |
| 10 | 9.75 | 225.450 | 416 | PASS | 308.1 | 416 | PASS |
| 0 | 9.75 | 222.713 | 416 | PASS | 317.2 | 416 | PASS |

Table 4-9 Custom cylinder capacity check, Tower Retraction.

| θ | Carrying Section (in) | x= 7.5 ft y = 5 ft | | | x= 4 ft, y = 4.5 ft | | |
|---|---|---|---|---|---|---|---|
| | | Force on Cylinder (kips) | Cylinder Capacity (kips) | PASS | Force on Cylinder (kips) | Cylinder Capacity (kips) | PASS |
| 0 | 9.75 | 6.343 | 226 | PASS | 8.3 | 226 | PASS |
| 10 | 9.75 | 70.245 | 226 | PASS | 92.2 | 226 | PASS |
| 20 | 9.75 | 121.279 | 226 | PASS | 159.5 | 226 | PASS |
| 30 | 9.75 | 158.683 | 226 | PASS | 209.2 | 226 | FAIL |
| 40 | 9.75 | 185.898 | 226 | PASS | 245.9 | 226 | FAIL |
| 50 | 9.75 | 205.006 | 226 | PASS | 272.6 | 226 | FAIL |
| 60 | 9.75 | 217.363 | 226 | PASS | 291.1 | 226 | FAIL |
| 70 | 9.75 | 223.941 | 226 | PASS | 303.2 | 226 | FAIL |
| 80 | 9.75 | 225.450 | 226 | PASS | 308.1 | 226 | FAIL |
| 90 | 9.75 | 222.713 | 226 | PASS | 317.2 | 226 | FAIL |

4.5 ENERGY CONSUPTION BY HYDRAULIC SYSTEM

Three different positions of hydraulic cylinder were tested for the prototype: 9 inches, 9.5 inches and 11 inches away from the prototype tower respectively. For each case the theoretical potential energy change and the actual electrical energy consumed by the system was calculated and recorded respectively. Finally, for each case the actual force on the hydraulic cylinder was calculated and energy consumption was also calculated using manufacturer's formulas. Multiple trials were conducted and the comparison between these energy values for different position can be seen in Table 4-10.

Table 4-10 Energy consumed by prototype system based on different approaches.

| Position | Connection At Wind Tower (in) | Connection of Cylinder on the Ground (in) | Theoretical Energy (J) | Average Electrical Energy consumed (J) | Energy Consumed Hydraulic Formulas (J) |
|---|---|---|---|---|---|
| 1 | 36.12 | 11 | 1333.01 | 14843.5 | 3326.19 |
| 2 | 36.12 | 9 | 1333.01 | 6540.5 | 1771.78 |
| 3 | 36.12 | 9.5 | 1333.01 | 5348.8 | 1940.9 |

Based on various positions of hydraulic cylinder connection, the following data has been collected. The amount of energy consumed by the hydraulic cylinder is directly proportional to the force produced by it or, the reaction induced on it. Therefore, the position in which the least reaction is generated is responsible for the least energy consumption. The actual electrical energy consumed is assumed to follow the general trend of the prototype i.e., 3.56 times the energy consumed calculated by hydraulic formulas.

The energy actual energy consumed by the hydraulic cylinder calculated using the industrial and manufactural specifications, the theoretical energy from gravitational formula is tabulated and finally, the actual electrical energy consumed based on the prototype is calculated and tabulated in Table 4-11.

Table 4-11 Energy consumed by wind tower erection system based on different approaches.

| Position | Connection At Wind Tower "x" (ft) | Connection of Cylinder on the concrete base "y" (ft) | Theoretical Energy (kJ) | Actual Energy Consumed (kJ) | Electrical Energy Consumed (kJ) |
|---|---|---|---|---|---|
| 1 | 7.5 | 5 | 2614.2 | 3414.71 | 12156.36 |
| 2 | 5 | 5 | 2614.2 | 4284.49 | 15252.79 |
| 3 | 4 | 5 | 2614.2 | 4354.29 | 15501.27 |
| 4 | 7.5 | 3 | 2614.2 | 7946.18 | 28288.36 |
| 5 | 3 | 5 | 2614.2 | 5863.0 | 20871.92 |

## 4.6 EQUATION TO DETERMINE CUSTOM HYDRAULIC CYLINDER SIZE FOR DIFFERENT TOWERS

In order to formulate an equation to determine the bore and pin size required for the custom hydraulic cylinder, two different cases were taken. For the first case, the Taper ratio of the wind tower was kept the same while the height of the tower was varied. Secondly, the taper ratio of the wind tower was varied with different sections, keeping the height of the tower constant. The following table 4-12 shows how the pin and bore size of the custom designed hydraulic cylinder are affected by the change in height of the wind tower.

Table 4-12 Hydraulic cylinder dimensions for constant taper ratio.

| Taper Ratio Constant = 0.01927 in/in | | | | | | |
|---|---|---|---|---|---|---|
| Height (ft) | Outer Radius (in) | Inner Radius (in) | Force Maximum (kips) | Pin Size (in) | Bore Size (in) | Allowable (in) |
| 97 | 30.6 | 8.157 | 225.6 | 2.64 | 7.57 | 8.23 |
| 90 | 30.6 | 9.775 | 208.8 | 2.59 | 7.29 | 8.23 |
| 85 | 30.6 | 10.932 | 196.5 | 2.55 | 7.07 | 8.23 |
| 80 | 30.6 | 12.088 | 183.9 | 2.51 | 6.84 | 8.23 |
| 70 | 30.6 | 14.400 | 158.3 | 2.42 | 6.34 | 8.23 |

The figure 4-10 shows the regression equations for the bore and pin size of the custom designed hydraulic cylinder considering a constant taper ratio of the wind turbine tower to be erected or lowered.
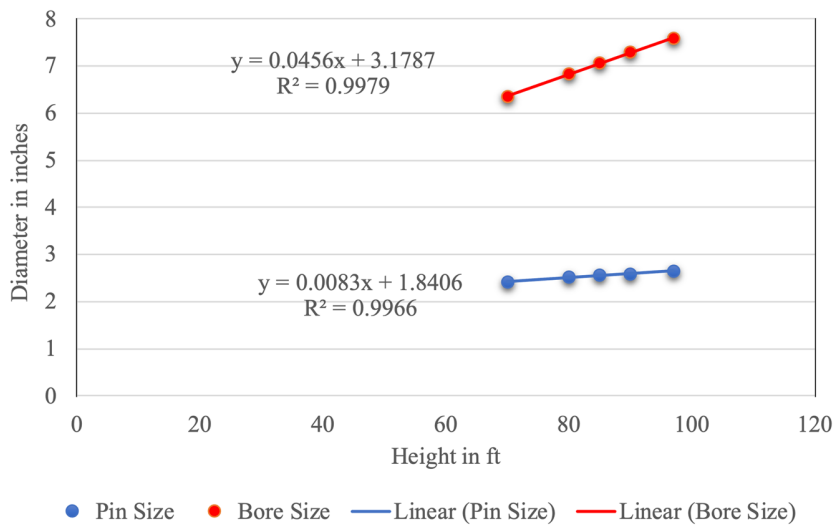


Figure 4-10 Size of custom cylinder required vs towers of varying height.

The following table 4-13 shows how the pin and bore size of the custom designed hydraulic cylinder are affected by the change in Taper ratio of the wind tower.

Table 4-13 Hydraulic cylinder dimension calculations, constant tower height.

| Height Constant H = 97ft | | | | | | |
|---|---|---|---|---|---|---|
| Taper Ratio (in/in) | Outer Diameter (in) | Inner Diameter (in) | Force Maximum (kips) | Pin Size (in) | Bore Size (in) | Allowable (in) |
| 0.01927 | 30.6 | 8.157 | 225.6 | 2.64 | 7.57 | 8.23 |
| 0.015 | 30.6 | 13.127 | 241.9 | 2.69 | 7.85 | 8.23 |
| 0.0214 | 30.6 | 5.678 | 217.5 | 2.62 | 7.44 | 8.23 |
| 0.01723 | 30.6 | 10.532 | 233.4 | 2.66 | 7.71 | 8.23 |
| 0.00909 | 30.6 | 20.006 | 264.5 | 2.75 | 8.21 | 8.23 |

The figure 4-11 shows the regression equations for the bore and pin size of the custom designed hydraulic cylinder considering a constant height of the wind turbine tower to be erected or lowered.
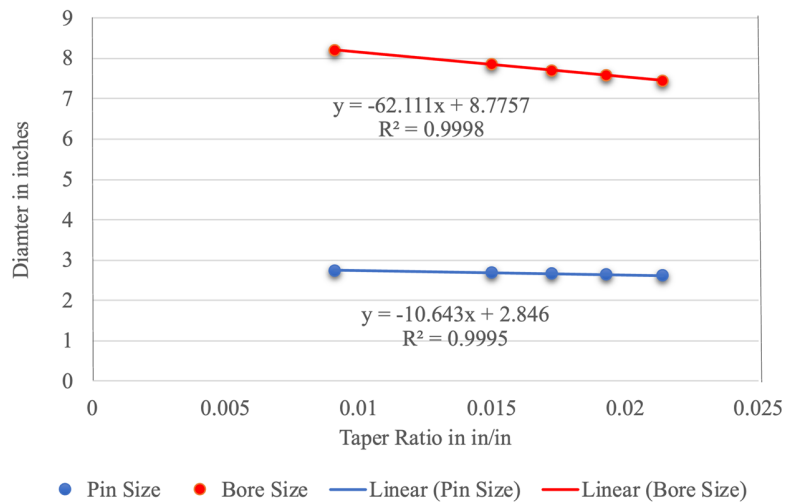


Figure 4-11 Size of custom cylinder required vs towers of varying taper ratio.

A detailed calculation showing the design of custom hydraulic cylinders can be found in Appendix B.

CHAPTER 5: **CONCLUSIONS**

5.1 SUMMARY

This thesis reveals crucial insights into optimizing hydraulic cylinder positioning for wind tower erection. Key findings emphasize the impact of connection height on the wind tower, constrained by hydraulic cylinder dimensions. Local cylinders prove unsuitable, necessitating custom solutions. Custom cylinders, similar in size to local ones, offer an effective optimization approach. While economic analysis is recommended for future research, these findings provide a foundation for enhancing wind tower erection efficiency and contributing to renewable energy infrastructure advancement.

5.2 CONCLUSIONS

In conclusion, this thesis has provided insights into the optimization of hydraulic cylinder positioning for wind tower erection. Through a comprehensive examination of the erection process, the key findings are:

- The height at which the connection is made significantly influences the ease of the erection process. However, this height is constrained by the dimensional restrictions of the hydraulic cylinders used in the operation. These limitations necessitate careful consideration when planning wind tower erection, as exceeding these restrictions could lead to operational challenges.

- Use of locally available hydraulic cylinders in the analysis revealed that they were unsuitable for the specific requirements of wind tower erection. This highlights the importance of selecting hydraulic cylinders that are specifically designed or customized to meet the demands of this task.

- Custom hydraulic cylinders, with dimensions similar to the locally available ones, can be manufactured to facilitate the erection process effectively. This finding opens possibilities for optimizing the equipment used in wind tower erection, potentially improving efficiency and safety.

- A connection at 7.5 ft from the base at the wind tower and 5 ft at the ground represents the most optimal position for connection, considering the dimensional constraints. In this case, $\alpha = 58°$ when the tower is fully lowered.

- For the case of a regular tower, where dimensional constraints allow, an $\alpha$ angle of 90° when the tower is fully lowered is identified as the most economical position.

5.3 LIMITATION OF STUDY

While this study has provided valuable insights into the optimization of hydraulic cylinder location for wind tower erection, it is necessary to recognize the inherent limitations that may influence the generalizability and comprehensiveness of the findings. By acknowledging these limitations, we gain a better understanding of the scope and applicability of the study's conclusions. These can guide future research and improve the engineering practices in wind tower construction and erection.

- Height of Connection: The decision to limit the height of the connection below 15ft was made to reduce wind effects, but this constraint might not fully reflect real-world scenarios. Wind patterns and intensities can vary significantly based on location and weather conditions. Therefore, the findings may be more applicable to specific regions with moderate wind conditions, and further investigation is needed to assess the system's performance under different wind scenarios.

- Simplified Calculations: Keeping the connection height below 15ft for ease of calculation might lead to oversimplifications in the analysis. Real-world wind tower erection projects often involve complex and dynamic forces, which were not fully considered in this study. More comprehensive numerical simulations or experimental testing would be beneficial to provide a more accurate representation of the system's behavior.

- Standardized Cylinders: The use of standardized cylinders was a practical choice to save costs and fabrication time. However, the limitations associated with these cylinders, such as size and force capacities, could affect the overall optimization process. Even the custom cylinder design on this thesis is based almost entirely on the range and dimensions preset by locally available hydraulic cylinders, assuming that the economic standpoint remains unchanged. Further research of the market is required to actualize this hypothesis.

- Simplified Wind Load Model: The study assumed a simplified wind load model to calculate the wind effects. This model may not fully capture the complexities of aerodynamic forces on the wind tower. Implementing more sophisticated wind load models could offer a more accurate representation of the wind-induced stresses and guide better design decisions.

- Contextual Generalization: The findings and conclusions of this study are based on the specific parameters and conditions considered for wind tower erection. Generalizing these results to other types of hydraulic systems or engineering applications may not be directly applicable without appropriate adjustments and validations for each specific context.

In summary, while this study provides valuable insights into the optimization of hydraulic cylinder location for wind tower erection, it is essential to recognize its limitations. Future research should address these limitations by incorporating more realistic wind conditions, considering custom cylinder solutions, refining stress analysis, exploring additional parameters, and validating the findings in practical applications to improve the overall understanding and applicability of the study's results.

## 5.4 RECOMMENATIONS

Based on the findings and limitations of this study, several key recommendations are proposed to enhance the optimization of hydraulic cylinder location for wind tower erection. These recommendations aim to address the identified limitations and build upon the study's insights to further improve the efficiency, safety, and sustainability of wind tower construction.

- Advanced Wind Load Analysis: To better capture the dynamic and complex nature of wind effects on wind towers, it is recommended to utilize advanced wind load analysis techniques. Computational Fluid Dynamics (CFD) simulations and wind tunnel testing can provide more accurate data on wind forces, allowing for a more precise assessment of the system's performance under varying wind conditions. This will lead to more informed decisions in positioning the hydraulic cylinder connection, ensuring robustness and resilience in the face of different wind patterns.

- Custom Cylinder Solutions: Although standardized cylinders were considered for cost-effectiveness, exploring custom cylinder solutions merits attention. Custom cylinders design discussed in the thesis is limited to a structural approach and would likely need to be taken into consideration from a mechanical point of view. Furthermore, hydraulic

energy efficiency needs to be field tested in order to provide a more accurate assumption of cost effectiveness.

- Field Validation: To ensure the practical applicability of the study's findings, it is essential to conduct field validation tests. Real-world wind tower erection projects should be monitored and evaluated using the optimized hydraulic cylinder locations proposed in this study. Field data collection will provide valuable feedback on the actual performance and effectiveness of the suggested optimization strategies, verifying their success in real-world scenarios.

- Cost-Benefit Analysis: While custom cylinders offer potential advantages, it is essential to perform a comprehensive cost-benefit analysis to assess their viability for each specific wind tower construction project. Evaluating factors such as initial costs, fabrication time, system performance improvements, and long-term maintenance will guide informed decisions on whether to opt for custom cylinder solutions.

In conclusion, these recommendations are put forth to guide further research and improve the implementation of hydraulic cylinder optimization for wind tower erection. Addressing the limitations and embracing these recommendations will contribute to the advancement of wind energy infrastructure, promoting sustainable and efficient wind tower construction practices in the pursuit of a greener and cleaner energy future.

# REFERENCES

Abdulla, N. (2021). A Strain model for uPVC tube-confined concrete. Cogent Engineering, 8. DOI: https://doi.org/10.1080/23311916.2020.1868695

Aggressive Hydraulics. (2023). Common Hydraulic Cylinder Formulas. AggressiveHydraulics.com. Retrieved Nov. 16, 2023, from https://www.aggressivehydraulics.com/resources/common-hydraulic-cylinder-formulas/

American Institute of Steel Construction. (2017). Steel Construction Manual (15th ed). Chicago, IL

Basu, B. (2010). Tower design and analysis. In WIT Transactions on State of the Art in Science and Engineering, 44(16). DOI: 10.2495/978-1-84564-205-1/16.

Bradford, M. A., & Gao, Z. (1992). Distortional Buckling Solutions for Continuous Composite Beams. Journal of Structural Engineering, 118(1). DOI: https://doi.org/10.1061/(ASCE)0733-9445(1992)118:1(73)

Calautit, K., Aquino, A., Calautit, J. K., Nejat, P., Jomehzadeh, F., & Hughes, B. R. (2018). A Review of Numerical Modelling of Multi-Scale Wind Turbines and Their Environment. Computation, 6(1), 24. DOI: https://doi.org/10.3390/computation6010024

Campione, G., Cannella, F., Zizzo, M., & Pauletta, M. (2021). Buckling strength of steel tube for lifting telescopic wind steel tower. Engineering Failure Analysis, 121, 105153. DOI: https://doi.org/10.1016/j.engfailanal.2020.105153

Chapple, P. (2002). Principles of Hydraulic System Design. Momentum Press. New York City, New York.

Cuong, B. H. (2021). Local buckling of thin-walled circular hollow section under uniform bending. Journal of Science and Technology in Civil Engineering (JSTCE) - HUCE, 15(4), 88-98. DOI: https://doi.org/10.31814/stce.huce(nuce)2021-15(4)-08

Flodraulic. (2018) Basic Hydraulic Formulas. Flodraulic.com. Retrieved Nov. 16, 2023, from https://flodraulic.com/formulae/basic-hydraulic-formulas/

Gao, Z., & Liu, X. (2021). An Overview on Fault Diagnosis, Prognosis and Resilient Control for Wind Turbine Systems. Processes, 9(2), 300. DOI: https://doi.org/10.3390/pr9020300

Hibbeler, R.C. (2017). Structural Analysis (10th ed.). Pearson. New York City, New York.

Hydraulics Online. (2018). About Hydraulic Cylinders. Hydraulicsonline.com. Retrieved Nov. 16, 2023, from https://hydraulicsonline.com/technical-knowledge-hub/about-hydraulic-cylinders/

ISO TS13725. (2001). Method of determining the buckling load: Hydraulic fluid power cylinders (ISO TS13725:2001). ISO.

Morelli, P. (2009). On the buckling behavior of telescopic hydraulic cylinders. KEM, 417–418, 281–284. DOI: https://doi.org/10.4028/www.scientific.net/KEM.417-418.281

Narvydas, E. (2017). Buckling strength of hydraulic cylinders - engineering approach and finite element analysis. Mechanika, 22(6). DOI: 10.5755/j01.mech.22.6.15374

Parrett, J. T., & Iyengar, S. K. R. (1976). "Buckling" Failure Assessment for Long Cylinders. SAE Technical Paper 760641. DOI: https://doi.org/10.4271/760641

Perch Energy. (2022, November). Residential Wind Turbines at Home. Perch Energy. Retrieved Nov. 16, 2023, from https://www.perchenergy.com/blog/energy/residential-wind-turbines-at-home

PowerX International. (2018). Choosing the Right Hydraulic Cylinder for a Lifting Application. PowerXInternational.com. Retrieved Nov. 16, 2023, from

https://powerxinternational.com/choosing-the-right-hydraulic-cylinder-for-a-lifting-application/

Valliappan, R., & Basha, A. (2017). Multistage Hydraulic Cylinder Buckling Analysis by Classical and Numerical Methods with Different Mounting Conditions. In Lecture Notes in Mechanical Engineering (pp. 901-910). DOI: https://doi.org/10.1007/978-81-322-2743-4_85

Rashad, H., Kamel, S., Jurado, F. (2017). Chapter 2 - The Basic Principles of Wind Farms. In
G.B. Gharehpetian & S. Mohammad Mousavi Agah (Eds.), Distributed Generation Systems (pp.
21-67). Butterworth-Heinemann. ISBN 9780128042083. DOI: https://doi.org/10.1016/B978-0-
12-804208-3.00002-9

Sørensen, J. D., & Sørensen, J. N. (Eds.). (2011). Wind Energy Systems: Optimising Design and
Construction for Safe and Reliable Operation (1st ed.). Woodhead Publishing. Sawston,
Cambridge.

Solazzi, L., & Buffoli, A. (2019). Telescopic Hydraulic Cylinder Made of Composite Material.
Applied Composite Materials, 26, 1189–1206. DOI: 10.1007/s10443-019-09772-8.

Sochacki, W. (2007). The dynamic stability of a laboratory model of a truck crane. Thin-Walled
Structures, 45(10–11), 927-930.DOI: https://doi.org/10.1016/j.tws.2007.08.023

Timoshenko, G.: Theory of Elastic Stability. McGraw hill publication (1963). New York City,
New York.

Trame, M., & Müller, S. (2015). Tower for a wind turbine and method of erecting a wind energy
tower (Patent No. EP3085956A1). Assignee: Nordex Energy SE and Co KG.

Tummala, A., Velamati, R. K., Sinha, D. K., Indraja, V., & Hari Krishna, V. (2015). A review on small scale wind turbines. Renewable and Sustainable Energy Reviews, 56, 1351-1371. DOI: 10.1016/j.rser.2015.12.027

U.S. Department of Energy. (2019). How Do Wind Turbines Work? U.S. Department of Energy. Retrieved Nov. 16, 2023, from https://www.energy.gov/eere/wind/how-do-wind-turbines-work

U.S. Energy Information Administration. (2019). Today in Energy. U.S. Energy Information Administration. Retrieved Nov. 16, 2023, from https://www.eia.gov/todayinenergy/detail.php?id=41474

U.S. Energy Information Administration. (2023). Electricity FAQs. U.S. Energy Information Administration. Retrieved Nov. 16, 2023, from https://www.eia.gov/tools/faqs/faq.php?id=97&t=3

von Ahn, P. (2012). Method for erecting a wind turbine tower. US Patent No. US2012/0304588A1.

Wangikar, S., Patil, A., & Patil, S. (2015). Design and Buckling Analysis of Multistage Hydraulic Lifter. International Research Journal of Engineering and Technology (IRJET), 02(08)

Wei, X., Jiang, Y., Zeng, W., & Pan, X. (2016). The coupling effects of the missile launcher and the ground in vehicle-mounted missile erecting. Advances in Mechanical Engineering, 8. URL: https://api.semanticscholar.org/CorpusID:114145398

Wind Power Engineering. (2016). Liebherr 1000 EC-B 125 Litronic tower crane used to erect turbine with 149 m hub height. Retrieved Nov. 16, 2023, from https://www.windpowerengineering.com/liebherr-1000-ec-b-125-litronic-tower-crane-used-erect-turbine-149-m-hub-height/

Wind Systems Magazine. (2016). Cranes and Wind Power: A Critical Pairing. Wind Systems Magazine. Retrieved Nov. 16, 2023, from https://www.windsystemsmag.com/cranes-and-wind-power-a-critical-pairing/

WindmillsTech. (2023). Wind Turbine Components. WindmillsTech. Retrieved Nov. 16, 2023, from https://windmillstech.com/wind-turbine-components/

Xiong-Hao, C., Duan-Wei, S., Shuang-Yang, Y., Xiang-Yu, Z., Zhi-Lin, S., Ji, Z., & Yang, L. (2017). Stability Analysis of Large Slenderness Ratio Horizontal Hydraulic Cylinder. IOP Conference Series: Materials Science and Engineering, 231. DOI:10.1088/1757-899X/231/1/012179.

APPENDIX A: STRUCTURAL ANALYSIS

CENTER OF GRAVITY CALCULATION

The unconventional shape and height of wind tower represents a non-uniform distribution of load along its length. However, for this research a single long truncated cylindrical shaped tower, with a uniform taper ratio is considered. Hence the load distribution is uniform along its length and the COG can be calculated based on its sectional view.
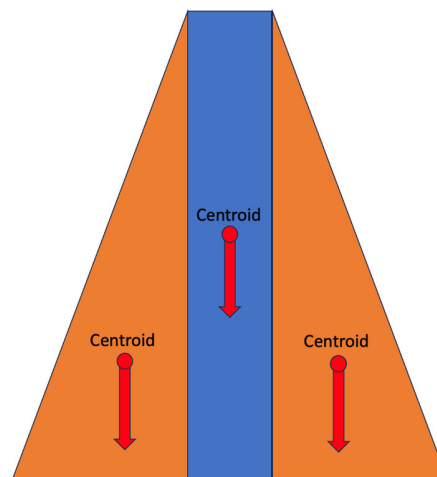


Figure A-1 Sectional view of tower

The determination of the center of gravity (COG) of the trapezoidal shape, consisting of two right-angled triangles attached back-to-back onto a rectangle when viewed from the front, was achieved using a straightforward method.

The shape was divided into its constituent components, namely the two right-angled triangles and the rectangle, and each component was assigned its own COG. The centroid of the right-angled triangles was calculated as the $\frac{1}{3}$ of the distance from the base. Meanwhile, the centroid of the rectangle was found by locating its center point, which was determined as the midpoint of its width and height. To account for the distribution of mass, each component was weighted based on its respective mass or area. The total mass or area of the entire trapezoidal shape was determined by summing the masses or areas of its individual components. Finally, the centroid coordinates of each component were multiplied by their corresponding mass or area and then divided by the total mass or area to calculate the weighted average COG.

$$COG = \frac{\sum y_{centroid} \times Area}{\sum Area} \qquad (A.1)$$

By following this methodology, the COG of the trapezoidal shape was accurately determined.

Table. A-1: Sample calculation for center of gravity

| Height of Tower | 97 | ft |
|---|---|---|
| Diameter at Base | 61.2 | in |
| Diameter at Top | 16.5 | in |
| Area of triangles | 433.6 | in$^2$ |
| Area of rectangle | 1598.3 | in$^2$ |
| centroid of triangle | 32.3 | ft |
| centroid of rectangle | 48.5 | ft |
| COG | 39.1 | ft |

Table A-2: COG for various wind tower configurations

| Height (ft) | COG (ft) | Taper Ratio (in/in) | COG (ft) |
|---|---|---|---|
| 97 | 39.14 | 0.01927 | 39.14 |
| 90 | 37.27 | 0.01500 | 42.04 |
| 85 | 35.79 | 0.02140 | 37.40 |
| 80 | 34.22 | 0.01723 | 40.61 |
| 70 | 30.80 | 0.00909 | 45.12 |

MOMENT DIAGRAM

Moment diagram of the entire system was an integral component. This allows us to determine the moment at the connection of the hydraulic cylinder and therefore the added load that the cylinder must carry. Moment diagram was created for each of the connection points from the range to check not only the force but also the structural integrity of the section at which the moment was being generated i.e., the section at which the cylinder was connected.

To find the moment diagram, first an equation of moment at a random distance "x" from the base of the tower must be generated. Firstly, the load distribution along the length of the tower is linearly varying as following.
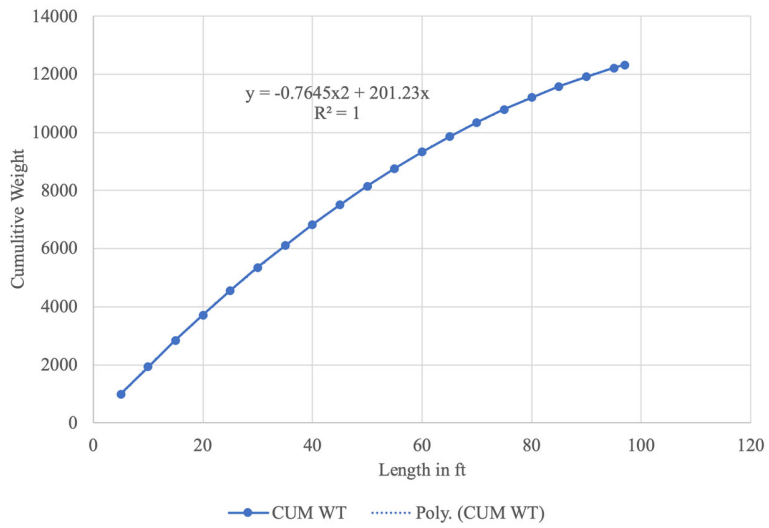
Figure A-2 Cumulative weight distribution graph for wind tower

Now considering that the tower is being erected or lowered as the line diagram below, we can formulate an equation of Moment at distance "x" from the base.
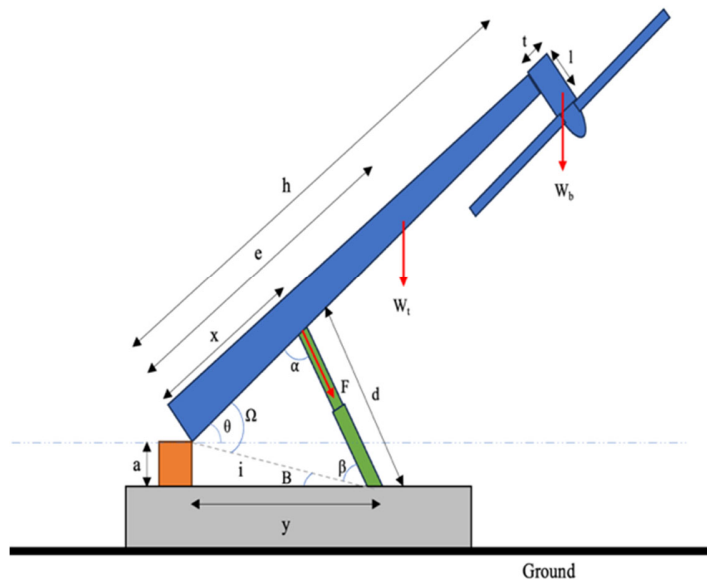


Figure A-3 2D Diagram showing wind tower erection with various angles.

The equation of Moment can be written as,

$$M_x = -R_y \cos \theta \times x + R_x \sin \theta \times x + w \times COG \times \cos \theta + F \sin \alpha \times (x - a) \qquad \text{(A.2)}$$

( NOTE: At θ = 90°,

$$M_x = -R_y \cos \theta \times x + R_x \sin \theta \times x + w \times COG \times \cos \theta + F \sin \alpha \times (x - a) - W_b l \sin \theta \,)$$

Referring to the following figure,

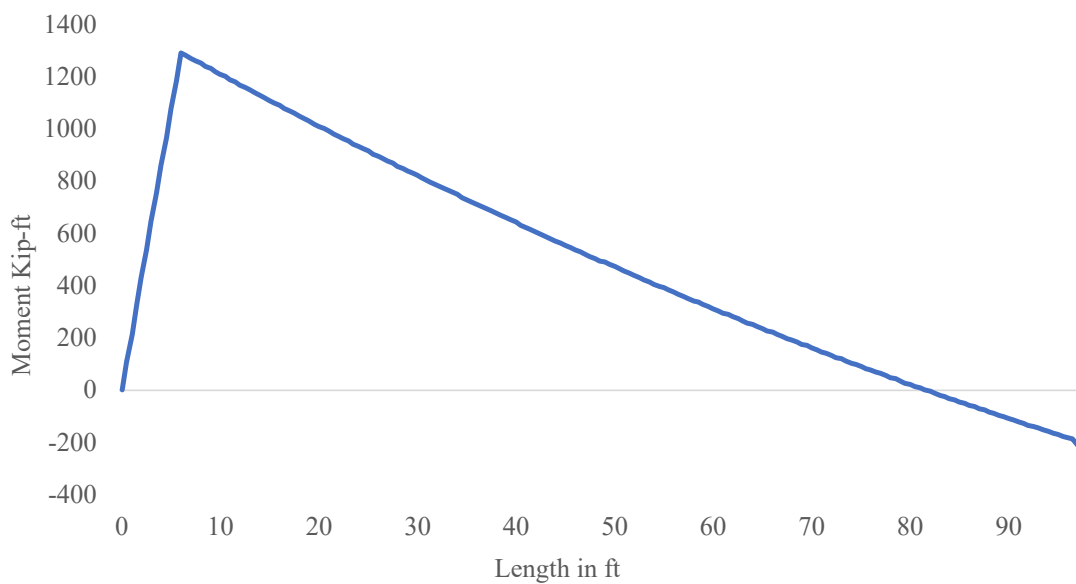AT "x" = 7.5ft and "y" = 5ft

MOMENT DIAGRAM AT VARIOUS ANGLES



Figure A-4 At θ = 0°

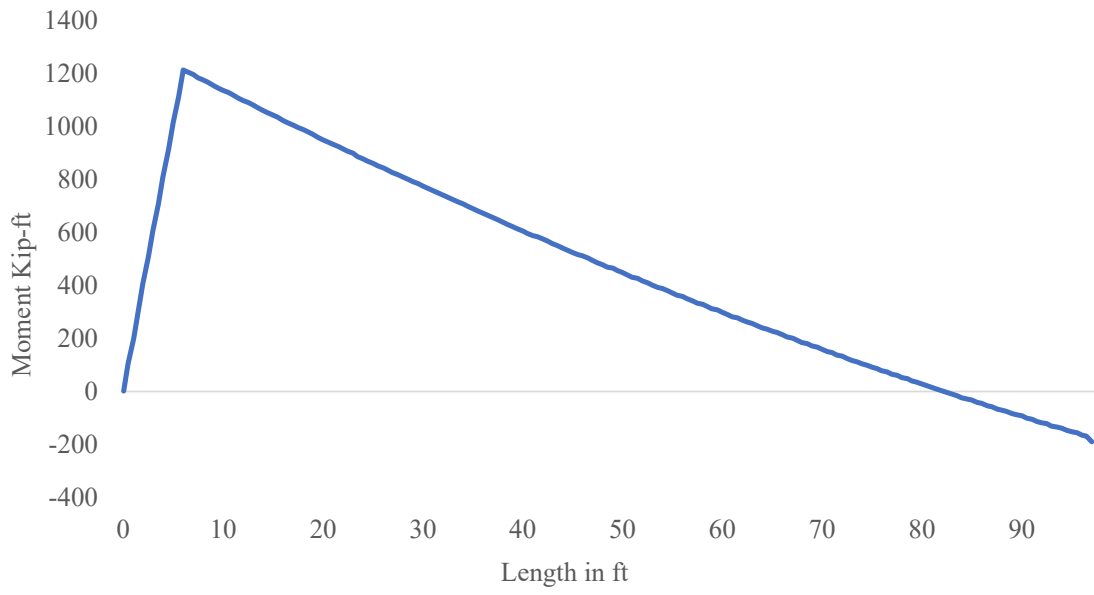Figure A-5 At θ = 20°
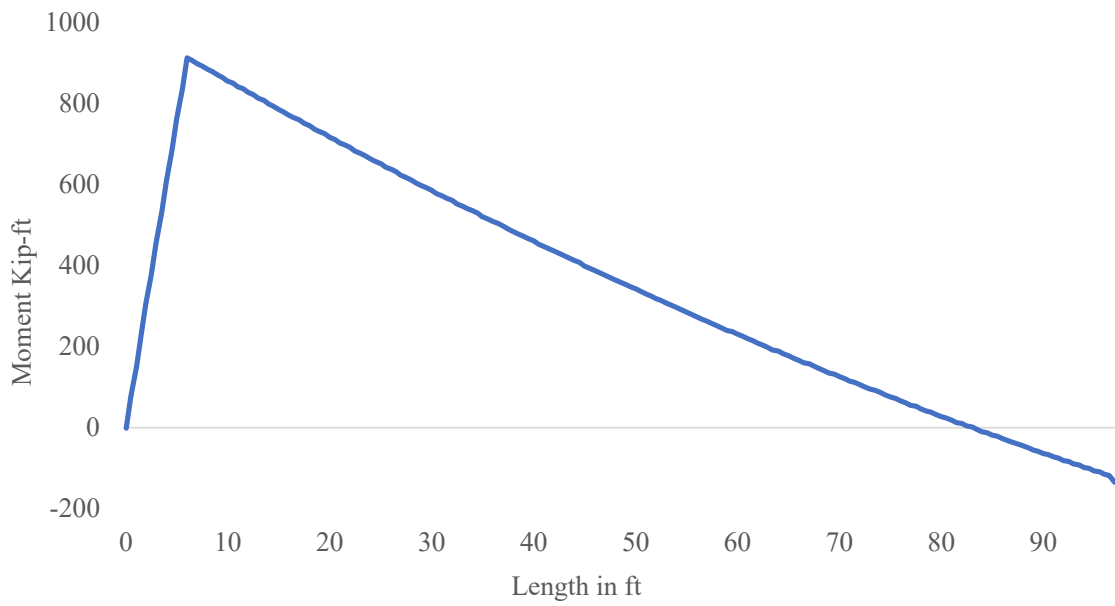


Figure A-6 At θ = 45°
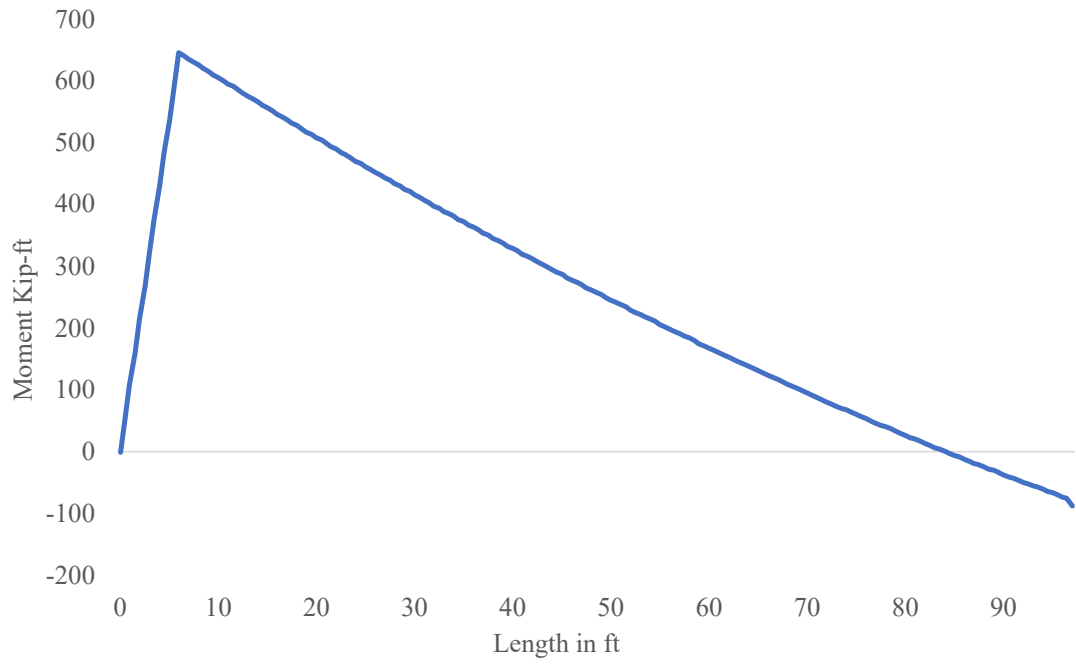
Figure A-7 At θ = 60°
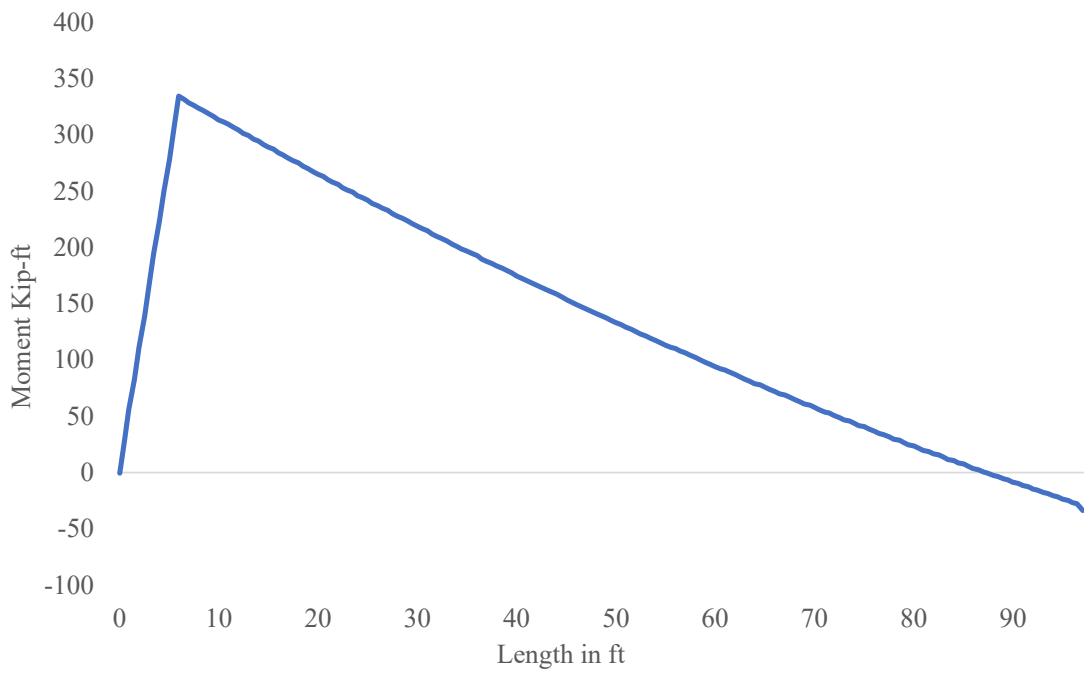


Figure A-8 At θ = 75°

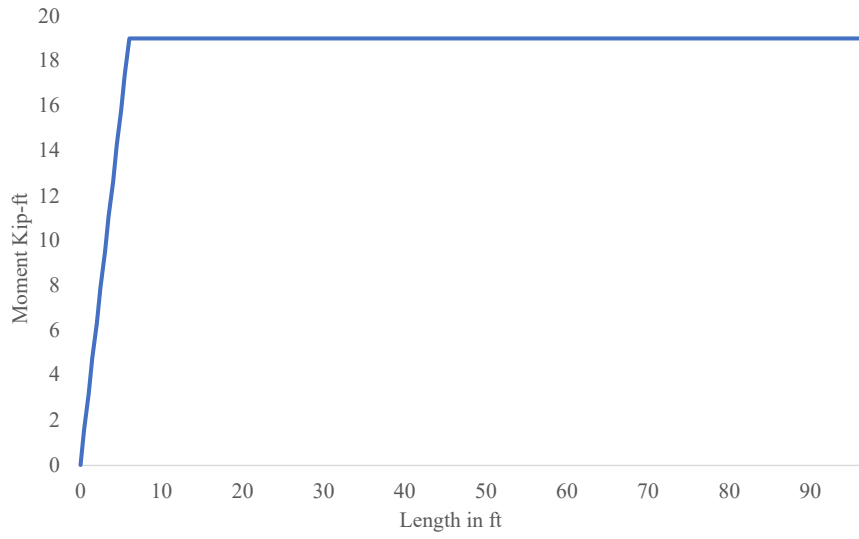Figure A-9 At θ = 90°

FORCE AND REACTION CALCULATION
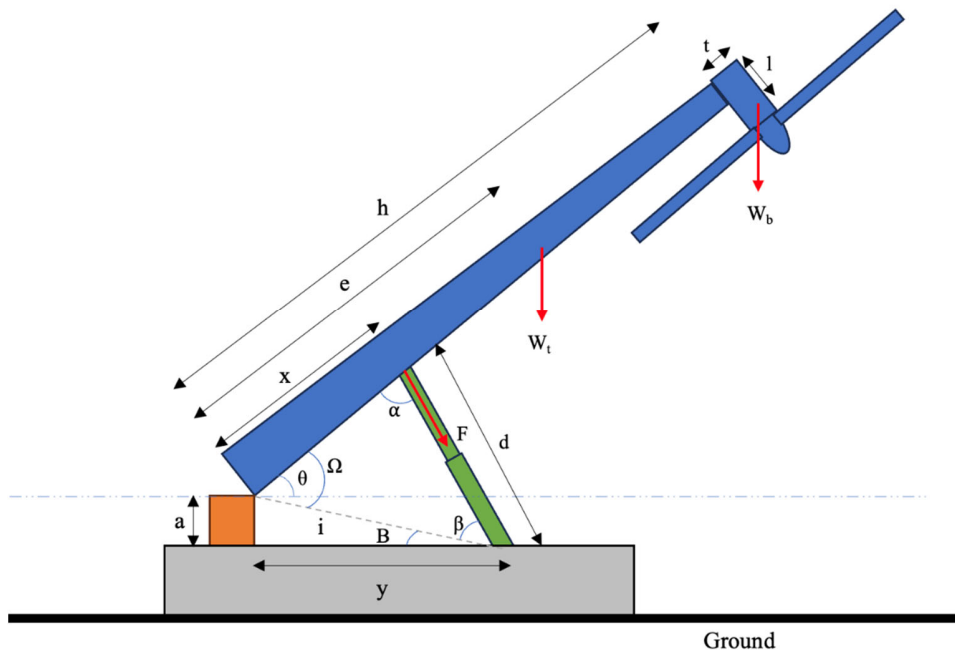


Figure A-10 2D Diagram of wind tower

89

$$\sum M_{hinge} = 0 \ (anti \ clockwise \ motion \ positive)$$

$$-Fsin\alpha.x - W_t \times ecos\theta - W_b \times \left(hcos\theta + lcos(90 - \theta)\right) = 0$$

$$F = -\frac{W_t \times ecos\theta + W_b \times (hcos\theta + lsin\theta)}{x \times sin\alpha}. \tag{A.3}$$

Similarly, $\sum F_y = 0$

$$R_y = W_t + W_b - F \times cos\alpha \times sin\theta - F \times sin\alpha \times cos\theta \tag{A.4}$$

Similarly, $\sum F_x = 0$

$$R_x = F \times sin\alpha \times sin\theta - F \times cos\alpha \times cos\theta \tag{A.5}$$

STRENGTH OF SECTION OF CONNECTION

In order to determine the controlling length of the connection, it must be compared to the maximum allowable shear strength and flexure strength that the section of connection possesses. For this, the distribution of weight along the length of the wind turbine must be determined.

We know, $W = \varrho \times V$

Since the volume of a hollow truncated cone can be written as,

$$V = h * \pi / 3 \times (R^2 + Rr + r^2 - S^2 - Ss - s^2) \tag{A.6}$$

Considering x to be an unknown height up to which the volume needs to be determined, this can be re-written as,

$$V_x = x \times \pi / 3 \times (R^2 + R * (R - 0.0192x) + (R - 0.0192x)^2 - (R - 0.311)^2 - (R$$
$$- 0.311)(R - 0.311 - 0.0192x) - (R - 0.311 - 0.0192x)^2$$

Therefore, the weight equation can be written as,

$$W_x = 0.282 * V_x$$

Shear strength per unit length can be determined by integrating this value up to required length. In this case, the length of connection.

$$V(x) = \int_0^x 0.282 * V_x$$

$$V(x) = 0.282 \times (x \times \pi / 3 \times (30.5875^2 + 30.5875 * (30.5875 - 0.0192x) + (30.5875$$
$$- 0.0192x)^2 - (30.5875 - 0.311)^2 - (30.5875 - 0.311)(30.5875 - 0.311$$
$$- 0.0192x) - (30.5875 - 0.311 - 0.0192x)^2)$$

$$V(x) = -0.00529x^2 + 16.76949x$$

But we know that the actual shear force at point of connection from base is given by,

$$V_x = R_{hinge} - \{-0.00529x^2 + 16.76949x\}$$

Using equilibrium equations, the Reaction at hinge can be calculated as following,

$$M_{hinge} = R_{cylinder} \times x - 12.329 \times 32.33 \times 12 - 9.629 \times 97 \times 12 = 0$$

$$R_{cylinder} = \frac{15991.316}{x}$$

$$Fy = 0 = R_{hinge} + R_{cylinder} - 12.329 - 9.629$$

$$R_{hinge} = 21.958 - \frac{15991.316}{x}$$

This, Vx can be re-written as,

$$V_x = 21.958 - \frac{15991.316}{x} - (-0.00529x^2 + 16.76949x)$$

Equating this with the maximum allowable shear strength of a section as calculated earlier we get,

$$21.958 - \frac{15991.316}{x} - (-0.00529x^2 + 16.76949x)$$

$$= \frac{22620}{\left(\frac{61.175 - 0.0.0192x}{0.311}\right)^{\frac{3}{2}}} \times (-0.03753x + 59.4853013)$$

Solving this equation we get, x = 3100 inches, which means that there is no shear failure at any point of connection.

Further integrating the shear equation gives the moment equation for the wind turbine,

$$M_x = \int_0^x V_x = \int_0^x R_{hinge} - \{-0.00529x^2 + 16.76949x\}$$

$$M_x = R_{hinge} \times x + \frac{0.00529x^3}{3} - 16.76949 \times \frac{x^2}{2}$$

$$M_x = 21.958x - 1599.316 + \frac{0.00529x^3}{3} - 16.76949 \times \frac{x^2}{2}$$

Equating this with the maximum allowable flexural strength of a section as calculated earlier we get,

Considering Yielding,

$$21.958x - 1599.316 + \frac{0.00529x^3}{3} - 16.76949 \times \frac{x^2}{2}$$

$$= 50 \, (0.000459x^2 - 1.45419x + 1152.453332)$$

Considering Local Buckling,

$$21.958x - 1599.316 + \frac{0.00529x^3}{3} - 16.76949 \times \frac{x^2}{2}$$

$$= \frac{2976.27}{61.175 - 0.0192x}$$

$$* \frac{-0.000028x^3 + 0.131572x^2 - 208.543042x + 110181.978524}{-0.0768x + 122.35}$$

For yielding condition the value of x reaches well beyond 4000 inches and for local buckling no solution exists, suggesting that at no point of the wind tower a section fails from local buckling or yielding.

The above solution presents the situation that the hydraulic cylinder can be connected anywhere in the wind turbine without having any issues of failure of the system. However, this cannot be the case, as we know that several other factors must be considered one major factor being the local availability.

$$A_g = \pi \, (R^2 - r^2) = \pi \, \{(30.5875 - 0.0192x)^2 - (30.5875 - 0.3111 - 0.0192x)^2\}$$

$$A_g = -0.03753x + 59.4853013$$

So, the maximum shear strength of section can be written as,

$$V_n = 0.6fy \times \frac{A_g}{2} = -0.56295x + 892.27952$$

For x= 120 inches, Nominal Shear strength is, $V_n = 824.72\ kips$

For a hollow circular section, since there is no weaker axis to undergo later torsional buckling and instead the section is governed by local buckling or yielding.

$$M_n = M_p = F_y Z \qquad\qquad (A.7)$$

where Z is the plastic modulus of the member's cross section.

And $\quad Z = \frac{4}{3}(R^3 - R_i{}^3) = \frac{4}{3} \times \{(30.5875 - 0.0192x)^3 - (30.5875 - 0.3111 - 0.0192x)^3\}$

$$Z = 0.000459x^2 - 1.45419x + 1152.453332$$

So, $M_n = 50\ (0.000459x^2 - 1.45419x + 1152.453332)$

Or Local buckling Strength,

Using AISC 15$^{th}$ edition, using table B4.1b to check if section is compact non compact or slender, considering a value of x = 50 inches

$$\frac{D}{t} = 181.825\ (as\ previously\ calculated)$$

$$for\ compact - non\ compact\ section. \frac{0.07E}{F_y} = 40.6$$

$$for\ non\ compact - slender\ sections. \frac{0.31E}{F_y} = 179.8$$

Since the section is slender,

$$M_n = F_{cr}S \tag{A.8}$$

We have,

$$Fcr = \frac{0.33E}{\frac{D}{t}} = \frac{2976.27}{61.175 - 0.0384x}$$

Also, S is the Elastic modulus of member cross section.

$$S = \frac{\pi}{4R}\left(R^4 - R_i{}^4\right) = \frac{\pi}{4(30.5875 - 0.0192x)}\{(30.5875 - 0.0192x)^4 - (30.5875 - 0.3111 -$$

$$0.0192x)^4\}$$

$$S = \frac{-0.000028x^3 + 0.131572x^2 - 208.543042x + 110181.978524}{-0.0768x + 122.35}$$

So nominal flexural strength is,

$$M_n = \frac{2976.27}{61.175 - 0.0384x}$$

$$\times \frac{-0.000028x^3 + 0.131572x^2 - 208.543042x + 110181.978524}{-0.0768x + 122.35}$$

Now checking both nominal flexural strength (yielding and local buckling) the controlling load can be determined. An example value of x = 120 inches can be taken, while keeping y value constant to check the controlling load.

For x= 120 inches, Nominal Flexural strength in yielding is,

$$M_n = 50 \ (0.000459x^2 - 1.45419x + 1152.453332) = 49228 \ kips - in$$

For x= 120 inches, Nominal Flexural strength in local buckling is,

$$M_n = \frac{2976.27}{61.175 - 0.0384x}$$

$$\times \frac{-0.000028x^3 + 0.131572x^2 - 208.543042x + 110181.978524}{-0.0768x + 122.35}$$

$$M_n = 40462.302863 \ kips - in$$

Therefore, the nominal flexural strength against local buckling is utilized for analysis.

BUCKLING CHECK FOR HOLLOW STEEL SECTION

A sample Buckling Check has been provided below for the worst-case scenario when the moment on the section will be the maximum to see if the section fails.

Table A-8 Stress and Buckling Test Sample Calculation

| Stress test | | | |
|---|---|---|---|
| 1 | Radius at x | 28.968 | in |
| 2 | MOI at x | 23371.7 | $in^4$ |
| 3 | Cross section Area at x | 2636.35 | $in^2$ |
| 4 | Moment at x | 227.63 | kip-in |
| 5 | Weight up to that point | 10954.665 | kips |

| 5 | Axial force up to that point | -5.8172 (compression) | kips |
|---|---|---|---|
| 6 | Stress | 0.284 | ksi |
| 7 | Stress test | PASS | |
| BUCKING TEST EULER's FORMULA | | | |
| 1 | K value | 2.1 | |
| 2 | length | 7 | ft |
| 3 | MOI at a | 23371.7 | in$^4$ |
| 4 | Euler's Force | 451.45 | kips |
| 5 | Axial force up to that point | -5.818 (compression) | kips |
| | | | |
| 6 | Buckling test | PASS | |
| BUCKLING TEST IN AISC FORMULA | | | |
| 1 | D/t | 186.293 | |
| 2 | Test | 237.273 | |
| 3 | CHECK | PASS | |
| 4 | Moment at x | 227.63 | kips-in |
| 5 | Plastic section Modulus | 519.172 | in$^3$ |
| 6 | Yielding Mn | 28554.415 | kip-in |
| 7 | Compact check | 163.455 | |
| 8 | SECTION TYPE | SLENDER | |
| 9 | Fcr | 51.371 | kips |
| 10 | ELASTIC SECTION MODULUS | 813.327 | in$^3$ |
| 11 | Mn Local Buckling | 41781.203 | kip-in |
| 12 | Controlling Moment (Mn) | 28554.415 | kip-in |
| 13 | TEST | PASS | |

# APPENDIX B: CYLINDER CALCULATIONS

OPTIMAL ENERGY CONSUMPTION

PROTOTYPE ANALYSIS

Since we cannot perform the experimental analysis to check the tower's erection and lowering time nor can we calculate the amount of voltage and current required for the whole process, calculating the actual energy required by the system is difficult to calculate.

Using the prototype described a relationship can, be generated for theoretical energy consumption, hydraulic energy and electrical energy consumed by the system. Using the potential energy equation, the theoretical energy was calculated as,

$$E = m \times g \times h = 1333.01\,J$$

Where, mass (m) is 45 lbs, Acceleration due to gravity (g) is 384 in/s$^2$ , height (h) is 32.94 in.

By experimental evaluation of voltage and current consumed the average energy consumed was calculated as (at connection on base 9.5 in),

$$E = 5348.8\,J$$

For hydraulic Energy Calculations,

The whole system took 29 seconds on average from the lowered position to get to the highest position.

$$Extend\ Time\ (sec) = \frac{(Extend\ Volume\ (in^3) \times 60)}{(Flow\ (gpm) \times 231)} \qquad (B.1)$$

Using this, the GPM was calculated as, 0.879 gallons per minute. Finally, the hydraulic power

can be calculated as,

$$HP = \frac{Pressure*GPM}{1714} = \frac{175.19\times0.879}{1714} = 0.0898 \ HP \tag{B.2}$$

Energy consumed by the hydraulic cylinder $= HP * \frac{29}{3600} = 0.000723 \ HP.hr = 1940.9 \ Joules$

WIND TOWER ANALYSIS

We know by the potential energy equation, the energy required by the wind tower to go from

fully lowered to a raised position can be calculated by,

$$E = m \times g \times h \tag{B.3}$$

$$E = m_{tower} * 386 * (39.140 * 12 - 0) + m_{turbine} * 386 * (97 * 12 - 0)$$

$$E = 2614196.185 \ Joules$$

Using the formula below and Table, we can use various positions and ranges to calculate the

Horsepower generated, with GPM = 12 given by manufacturers.

$$HP = \frac{Pressure * GPM}{1714} = \frac{1510.74}{1714} = 10.58 \ HP$$

The extend time is thus calculated as 216.303 seconds using equation B.1 as above.

Energy consumed by one hydraulic cylinder $= HP \times \frac{216.303}{3600} = 0.504 \ HP.hr = 1707354.425$

Joules

So, total energy consumed = 3414708.851 Joules.

Energy consumption is also dependent upon force generated on hydraulic cylinder, so x= 7.5ft and y = 5ft is still the most energy efficient positum for the hydraulic cylinder given the conditions.

The telescopic cylinder however fails to carry the load while retracting. In fact, most if not all locally available cylinders are not made for such a tedious task. As shown by the table, each cylinder has a large rod which significantly decreases its retracted area and hence its load carrying ability. A need for designing custom hydraulic cylinder arises because of this issue.

CUSTOM HYDRAULIC CYLINDER DESIGN

In order to keep the economical discrepancy to a minimum, the same range calculated for the locally available telescopic cylinder. For the most economical position, the load calculated during maximum capacity was taken as a standard load the cylinder must be able to carry. Also, the length was kept the same and the diameter of the cylinder was also made to uphold the criteria set above.

Having known the maximum loading on the cylinder using the optimum value previously calculated we can thus use this value as the critical buckling load of the custom Hydraulic cylinder and reverse engineer the custom hydraulic cylinder. Using the formula,

$$P_{cr} = \frac{\pi^2 \times E \times I}{nL_e} \tag{B.4}$$

when $\lambda > \lambda_{cr}$

Where, slenderness ratio ($\lambda = \frac{4L_k}{d}$), and $\lambda_{cr}$ is the critical slenderness ratio ($\lambda_{cr} = \pi\sqrt{\frac{E}{0.8R_e}}$) and

$R_e$ = the yield strength, d = piston rod diameter. Considering the cylinder connected with hinge connection on both ends, $L_k = 1 * Le = 5.05$ ft (length from previous locally available cylinder at lowered condition)

$$P_{cr} = \frac{\pi^2 \times E \times I}{nL_e}$$

$$\frac{225.5}{2} \, kips = \frac{\pi^2 \times E \times I}{nL_e} = \frac{\pi^2 \times 29000 \times \pi \times d^4}{1.2 \times 5.05 \times 64}$$

Considering a safety factor of 1.2, $d = 2.64 \, inches$

Selecting the bore size involves ensuring the retracted area of the cylinder can still carry the maximum load produced on the cylinder. We can simply use the 3000 psi common rating of hydraulic cylinders to generate the bore size.

$$A_{bore} \times STRENGTH = FORCE \qquad\qquad (B.5)$$

$$A_{bore} \times 3000 = 1.2 \times \frac{225.5}{2} \, kips$$

$$A_{bore} = 45.1 \, in^2$$

The diameter of the bore can thus be calculated as $D = 7.35"$ Which can also be taken as 7.5", however it is important to check if there is enough connection space available at that length of the tower for two such cylinders to be connected.

$$D_{allowable} = \frac{\left[\frac{D - 0.0384x}{2.5} - 2.5\right]}{2.5}$$

At x = 8.23 ft

$$D_{allowable} = 7.5 \ inches$$

a value of $D = 7.5 \ inches$ is taken.

Now to check if the retract area will be able to accommodate the maximum load,

$$F = 2 * 3000 * \left(\pi * \frac{D^2 - d^2}{4}\right) = 232.3 \ kips$$